R. & M. No. 3627

R. & M. No. 3627

MINISTRY OF TECHNOLOGY

AERONAUTICAL RESEARCH COUNCIL
REPORTS AND MEMORANDA

Further Experimental Investigations of Compressible Turbulent Boundary Layers with Air Injection

By L. C. SQUIRE

Cambridge University Engineering Department

LONDON: HER MAJESTY'S STATIONERY OFFICE
1970
PRICE £1 1*s.* 0*d.* [£1·05] NET

Further Experimental Investigations of Compressible Turbulent Boundary Layers with Air Injection

By L. C. SQUIRE

Cambridge University Engineering Department

Reports and Memoranda No. 3627*
August, 1968

Summary.

This report gives further experimental results for compressible turbulent boundary layers with air injection. The experimental arrangement is similar to that used by Jeromin (R. & M. 3526) but, by a slight modification of the injection equipment, and by a reduction in Reynolds number, it has been possible to obtain a threefold increase in injection rate at a Mach number of 2·5. Results were also obtained for a Mach number of 1·8. The basic velocity profiles are included in tabular form together with some of Jeromin's results for a Mach number of 3·6.

The present results, together with results for incompressible flow, have been used to study the law of the wall, the velocity defect law, and the eddy viscosity variation through the layer.

LIST OF CONTENTS

*Replaces A.R.C. 30 437.

---

1. *Introduction.*

In a recent report Jeromin[1] has presented experimental results for the compressible turbulent boundary layer on a flat porous surface with air injection at the surface. Results were given for a Mach number of 2·5 at various injection rates up to $\frac{\rho_w v_w}{\rho_1 U_1} = 0{\cdot}0013$, and at a Mach number of 3·6 for injection rates up to $\frac{\rho_w v_w}{\rho_1 U_1} = 0{\cdot}0021$. At the highest injection rate at $M = 3{\cdot}6$ the boundary layer appeared to be on the point of 'blow-off'. When the present author started a more extensive analysis of these results it became apparent that more results were needed, in particular results for higher injection rates at $M = 2{\cdot}5$, and some results at a lower Mach number to provide a link with incompressible results.

These additional results are presented in the present report. They were obtained from the same experimental equipment as used by Jeromin[1]. However, it was found that the injection mass flow was limited by the cooling equipment used by Jeromin. This cooling equipment was designed to enable the temperature of the injected air to be varied from about 15°C below the recovery temperature to about 15°C above (i.e. no cooling). In general, Jeromin's results showed very little effect of this small range in temperature on the overall results, and so it was decided to by-pass the cooling system in the new tests. The injection air was now taken directly from the tunnel high pressure air supply. This gave a 70 per cent increase in the available mass flow, but meant that the injection air was at a temperature close to the tunnel stagnation temperature, i.e. about 12°C above the plate recovery temperature (= 0°C). The actual mass flow rate $\left(\text{i.e.} \frac{\rho_w v_w}{\rho_1 U_1} \right)$ was then further increased by reducing the tunnel Reynolds number from about $1{\cdot}5 \times 10^7$ per foot, as used by Jeromin, to $0{\cdot}9 \times 10^7$ per foot. These changes gave a maximum injection rate of $\frac{\rho_w v_w}{\rho_1 U_1} = 0{\cdot}0036$ at $M = 2{\cdot}5$. Results were also obtained at a Mach number of 1·8 for injection rates up to 0·0031, using a new liner which was not available during the original tests.

The basic results of these tests are presented in tabular form. Some of Jeromin's velocity profiles for $M = 3{\cdot}6$ are also included for completeness.

The present results are analysed, together with those of McQuaid[2] for incompressible flow, and those of Jeromin for $M = 3{\cdot}6$ in the latter part of the report. This analysis deals with the overall effects of injection, the velocity defect law, and shear stress and eddy viscosity distributions. The analysis pertaining to the law of the wall has been published separately (Ref. 3).

2. *Details of Test.*

2.1. *Experimental Arrangement.*

The experiments were made in the intermittent blowdown supersonic tunnel in the Cambridge University Engineering Department. The experimental arrangement was basically the same as that used by

Jeromin[1], and so only a brief description will be given here. A photograph of the tunnel test section with the injection equipment is shown in Fig. 1, and a sketch of the injection section and the pitot traverse is shown in Fig. 2. The injection air was taken from the tunnel air supply at a pressure of about 14 atmospheres. It then passed through a reducing valve, which also acted as a mass-flow control device, and a filter. It was metered by a calibrated orifice, and entered the plenum chamber below the porous surface by means of the two inlets shown in Fig. 2. Baffle plates were placed above the inlets to break up the jets, and the air passed through another porous plate before entering the final plenum chamber directly below the porous surface. The pressure in this final chamber was virtually constant, and had a maximum value of about 2 atmospheres absolute at the maximum injection rates.

The injection surface used corresponds to plate A of Jeromin's paper. It was made of sintered bronze with a rolled surface (maximum particle diameter to pass was $2\frac{1}{2}$ microns). The plate was instrumented with thermocouples along the whole length. This particular plate had the largest pressure drop for given mass flow of the several plates which were available and was chosen in order to minimise variations in the injection mass flow caused by small variations in the static pressure along the plate. However, the actual porosity of the plate varies by ± 5 per cent for different positions on the surface.

The pitot pressures were measured by means of the traverse gear shown in Fig. 2. It was operated manually and enabled a complete boundary-layer traverse to be measured during a tunnel run of about 60 seconds. The pitot tube holder was strengthened by fins to allow measurements at various stations along the plate (*see* Jeromin for full details of the probe). The position of the probe relative to the wall was measured by a wiper sliding over a calibrated potentiometer. The pitot pressure was measured by a pressure transducer with a measuring range of 0 to 5 atmospheres. This arrangement allowed a continuous plot of pitot pressure against position to be obtained in a single run.

The pitot tube had a flattened mouth with an overall height of 0·0064 inches.

Wall temperature and tunnel stagnation temperature were recorded throughout the tunnel run, and the stagnation pressure and injection mass flow were maintained at constant values.

2.2. *Range of Tests.*

Boundary-layer traverses were made at Mach numbers of 2·5 and 1·8 for three injection rates. Traverses were also made on a solid surface at the same Mach numbers. The actual tests conditions are shown in the following table. The test conditions for Jeromin's tests at $M = 3{\cdot}6$ are again included for completeness.

Table of Test Conditions.

Nominal Mach number	1·8	2·5	3·6
Stagnation Pressure	26·7 psia	44·7 psia	119·7 psia
Stagnation Temperature	293°C	293°C	294°C
Reynolds Number per foot	$8{\cdot}0 \times 10^6$	$9{\cdot}7 \times 10^6$	$1{\cdot}51 \times 10^7$
Injection Rate $(\rho_w v_w/\rho_1 U_1)$	0 0·0013 0·0025 0·0031	0 0·0013 0·0024 0·0036	0 0·00065 0·0012 0·0021

Note that the stagnation temperature varied slightly from run to run—the maximum variation being ± 4°C. For the tests at $M = 1{\cdot}8$ and 2·5 the wall temperature was usually 2°C below the stagnation temperature, and at $M = 3{\cdot}6$ it was about 6°C below the stagnation temperature.

For all Mach numbers the boundary-layer traverses covered a distance of 5 inches along the surface.

The first station was 8·6 in. downstream of the leading edge of the porous plate (12 in. from the nozzle throat). In general traverses were made at inch intervals along the plate, but at $M = 2{\cdot}5$ some layers were measured at half-inch intervals. For convenience the possible eleven measuring stations are numbered 1 to 11. Station 1 corresponds to the most upstream position.

2.3. *Reduction and Accuracy of Results.*

The raw data was obtained as $X-Y$ charts of pitot-pressure-transducer reading against distance from the wall. A typical chart is shown in Fig. 3. This chart also recorded the wall temperature during the run. The tunnel stagnation temperature was recorded on another chart.

The chart for pitot pressure shows that the pressure is initially constant, but then changes suddenly as the pitot tube leaves the wall. It is estimated that this point can be determined from the chart to an accuracy of about 0·001 in. The charts were read manually to give about 30 readings through the boundary layers. These values were fed directly to a digital computer, together with calibration factors, atmospheric pressure and wall temperature. The calculated pitot-pressure profiles were then converted to Mach number profiles by the normal compressible flow relationships. Jeromin's tests have shown that the static temperature is related to the velocity ratio by the formula

$$T = T_w+(T_r-T_w)\left(\frac{u}{U_1}\right)-(T_r-T_1)\left(\frac{u}{U_1}\right)^2,$$

This formula was therefore used together with the Mach-number profiles to determine the velocity profiles by an iterative scheme. Once the velocity profile, and hence the density profile, was found the displacement and momentum thickness of the boundary layer were determined by numerical quadrature using a simple trapezium rule.

In general it was easiest to read the charts by finding the transducer reading at various grid-line values of y. Since the wall position did not always correspond to a grid-line this meant that the actual y positions varied for each profile. In order to produce convenient tables of the results a sub-programme was written which took the results as computed and interpolated the values of u/U_1 for fixed values of y. Cubic interpolation was used near the wall, but linear interpolation was used in the outer part of the layer. The resultant tables are presented in Tables 1 to 12.

Fig. 3 shows that the line of transducer reading against position does have a certain amount of vibration or noise. However, it was found that the mean value could usually be read to an accuracy of $\pm 0{\cdot}1$ small divisions of the grid. The actual values of u/U_1 corresponding to the pitot readings are also plotted on Fig. 3, and these show that the reading error in transducer output corresponds to an error of $\pm 0{\cdot}0008$ in u/U_1 near $u/U_1 = 1$, but to an error of $\pm 0{\cdot}005$ at $u/U_1 = 0{\cdot}40$. Other errors tend to be smaller than these direct reading errors.

It is estimated that the quoted injection rates are accurate to ± 5 per cent.

3. *Presentation of Results.*

The basic velocity profiles are tabulated in Tables 1 to 8. These tables also include the corresponding values of momentum and displacement thicknesses. For completeness Tables 9 to 12 contain velocity profiles for $M = 3{\cdot}6$ as measured by Jeromin*. These tables were obtained by interpolation from the calculated results and so may contain slightly larger errors than those quoted in the last section.

All the profiles are plotted as u/U_1 against y/θ in Figs. 10 to 12, while some sample profiles are plotted against y/δ in Figs. 6 to 8. These results are discussed below. It should be noted that these figures were plotted from the original calculated results and not from the interpolated values quoted in the tables.

In general all results discussed for Mach numbers of 1·8 and 2·5 are those obtained by the present author, whereas those for $M = 3{\cdot}6$ were obtained by Jeromin. The incompressible results were obtained by McQuaid[2].

*Jeromin did not include tabulated velocity profiles in his original report.

4. *Discussion of Results.*

4.1. *Effects of Injection on External Mach Number.*

The Mach-number distributions outside the boundary layer in the region of the boundary-layer measurements are shown in Fig. 4. These Mach numbers were obtained from the pitot readings in the free stream. It will be seen that the general effect of injection is to reduce the free-stream Mach number. At $M = 3{\cdot}6$ there is no change in the shape of the distribution, but at $M = 2{\cdot}5$ there are severe disturbances with injection at stations downstream of Station 3. These disturbances are less marked at $M = 1{\cdot}8$ but are still present. It is thought that these disturbances originate from the sudden thickening of the boundary layer at the start of injection. These disturbances pass downstream of the measuring stations at $M = 3{\cdot}6$. In view of these disturbances most of the analysis has been concentrated on the front stations at $M = 1{\cdot}8$ and $2{\cdot}5$. However, the effect of these disturbances is briefly discussed below (Section 4.2).

4.2. *Overall Effects of Injection.*

Figs. 6 to 8 show velocity profiles against y/δ (δ is boundary-layer thickness defined as the distance from the wall at which $u/U_1 = 0{\cdot}995$) for Mach numbers of $1{\cdot}8$, $2{\cdot}5$ and $3{\cdot}6$, while Fig. 5 shows similar profiles for incompressible flow. As is now well known the effect of injection is to make the profile less full and hence to reduce the skin friction at the wall. In general it was found that the effect of injection was almost linear with $\dfrac{\rho_w v_w}{\rho_1 U_1}$ (or F in the usual notation). This is illustrated in Fig. 9 where u/U_1 at $y/\delta = 0{\cdot}15$ is plotted against F for the profiles of Figs. 5 to 8. As will be seen the points all lie on straight lines, the slopes of which increase with increasing Mach number.

Results for Stations 1, 3, 5, 7, 9 (and 11) are plotted against y/θ in Figs. 10 to 12 for Mach numbers of $1{\cdot}8$, $2{\cdot}5$ and $3{\cdot}6$ respectively. For the solid plate ($F = 0$) the profiles for each Mach number collapse on to a single curve. With blowing the collapse is less impressive, although still very good at $M = 3{\cdot}6$, except for the last two stations at $F = 0{\cdot}0021$ where the boundary layer is on the point of 'blow-off'. (*See* Jeromin for more discussion of this point). The scatter is worse for the results at $M = 2{\cdot}5$, where, it will be remembered, there is a large disturbance in the external Mach-number distribution with blowing. Fig. 13 shows a comparison of the external Mach-number distribution at $M = 2{\cdot}5$, with the corresponding values of u/U_1 at $y/\theta = 1{\cdot}5$. The correspondence between the shapes of these curves suggests that the scatter in Fig. 11 is entirely due to the variations in external Mach number. Also the good agreement for the profiles at Stations 1 and 3 suggest that these profiles are virtually unaffected by the disturbances.

4.3. *Skin-Friction Results.*

The skin-friction coefficients were deduced from the measured boundary-layer developments by means of the momentum integral equation

$$\frac{d\theta}{dx} = \frac{C_f}{2} + F + \frac{\theta}{\rho_1 U_1^2}\frac{dp}{dx}(2 + H - M_1^2). \tag{1}$$

Measured momentum developments are shown in Fig. 14. The variations of θ with x are almost linear, and so $d\theta/dx$ was found by fitting a least-squares straight line through the points. The skin-friction coefficient could then be obtained directly from equation (1). For all the developments at $M = 3{\cdot}6$, and for zero blowing at $M = 1{\cdot}8$ and $2{\cdot}5$ this method gave satisfactory values of C_f. However, for the developments with blowing at $M = 1{\cdot}8$ and $2{\cdot}5$ the pressure-gradient term varied significantly along the surface and so gave wide variations in C_f along the surface. Since $d\theta/dx$ was assumed constant it was felt that these variations were unrealistic and so skin friction was determined by an alternate method. Equation (1) was rewritten as

$$\frac{d}{dx}(\theta - \theta_p) = \frac{C_f}{2} + F, \tag{2}$$

where $$\theta_p = \int_0^x \frac{\theta}{\rho_1 U_1^2} \frac{dp}{dx}(2+H-M^2)\,dx\,.$$

The least-squares slope of $(\theta-\theta_p)$ was then used to find C_f from equation (2).

Values of the skin-friction coefficients for all the profiles are tabulated in Table 13. The values in brackets show the values of skin-friction coefficients obtained by ignoring the pressure gradient term in equation (1).

Results for zero blowing are plotted in Fig. 15 against R_θ, where θ is the momentum thickness at the middle station (Station 6). This figure also includes values of C_f as obtained by other workers using skin-friction balances. The present results for $M = 1{\cdot}8$ and $2{\cdot}5$ are in good agreement with the balance measurements. However, the results for $M = 3{\cdot}6$ appear high. Jeromin assumed that this was due to three-dimensional effects and so reduced all his results at $M = 3{\cdot}6$ by $0{\cdot}0002$. These 'corrected' results are included in Table 13.

4.4. *Velocity Defect Law.*

For near-equilibrium turbulent boundary layers in incompressible flow McQuaid[7] showed that the outer part of the boundary layer could be expressed in the form

$$\frac{u-U_1}{U_*} = f(y/\delta)\,, \tag{3}$$

where $f(y/\delta)$ is a universal function, and

$$\begin{aligned} U_* &= U_1\,(d\theta/dx)^{\frac{1}{2}} \\ &= \left(U_\tau^2 + v_w\,U_1 - (2+H)\,\theta\,U_1 \frac{dU_1}{dx} \right)^{\frac{1}{2}}. \end{aligned} \tag{4}$$

Thus $U_* = U_\tau$ for zero pressure gradient and zero injection. The direct extension of this result to compressible layers is to write

$$\begin{aligned} U_* &= U_1 \left(\frac{T_w}{T_1} \frac{d\theta}{dx} \right)^{\frac{1}{2}} \\ &= U_1 \left(\frac{T_w}{T_1} \left(\frac{C_f}{2} + F + \frac{\theta}{\rho_1 U_1^2} \frac{dp}{dx}(2+H-M^2) \right) \right)^{\frac{1}{2}} \end{aligned} \tag{5}$$

since this again reduces to $U_* = U_\tau$ in the absence of injection and pressure gradient. Fig. 16a, taken from McQuaid's report, shows incompressible results in zero pressure gradient plotted in the ordinates of equation (3). As will be seen all the results for various blowing rates collapse on to a single curve. The line through the points correspond to the velocity defect on a solid surface for $R_\theta = 5 \times 10^4$ as given by Thompson's velocity profile family. This same line is also drawn in Figs. 16b, c and d which show the present results for Mach numbers of $1{\cdot}8$, $2{\cdot}5$ and $3{\cdot}6$ respectively. Again results for all blowing rates collapse on to the same curve. The results used to plot Figs. 16b to d were taken from Station 3, i.e. they correspond to the profiles plotted in Figs. 6 to 8. However, since Figs. 10 to 12 show that in constant pressure gradient the velocity profiles are similar at each station, it appears that all the present results could be collapsed on the same curve as drawn in Fig. 16a to d. Since equations (3) and (5) collapse the outer part of the profiles on to a single curve it is of interest to study this velocity defect law for solid surfaces, when the law reduces to

$$\frac{u-U_1}{U_\tau} = f(y/\delta)\,.$$

Fig. 16e shows the results obtained by Coles[4] for Mach numbers up to 4·55. It will be seen that the results for $M = 1{\cdot}98$ and $2{\cdot}57$ lie very close to the mean line of the previous figures. However, at $M = 3{\cdot}7$ the results lie above this line, and the discrepancy increases at $M = 4{\cdot}55$. These results suggest that $f(y/\delta)$ varies with Mach number above about $M = 3{\cdot}0$. In this case the present results for $M = 3{\cdot}6$ are called into question since they appear lower than Coles' results for $M = 3{\cdot}7$. However, it should be noted that present results for $M = 3{\cdot}6$ were obtained in a slight adverse pressure gradient which tends to increase the velocity defect. Thus the collapse of the present results for $M = 3{\cdot}6$ on to the same curve as for the lower Mach numbers may be fortuitous. However, there is no doubt that the present defect law collapses results for all blowing rates at constant Mach number.

4.5. *Shear-Stress Distributions.*

Originally it was intended to derive the shear-stress distributions through the layer from the velocity developments by integration of the equations of motion, that is, from

$$\tau = \tau_w + y\frac{dp}{dx} + \int_0^y \frac{\partial}{\partial x}(\rho u^2)\,dy - u\int_0^y \frac{\partial}{\partial x}(\rho u)\,dy + \rho_w v_w u\,. \tag{6}$$

A computer programme to evaluate τ from this relation was written, but it was found that the resultant shear-stress profiles varied wildly along the plate. This variation could be reduced slightly by smoothing the measured values of u (or u/U_1) at constant y, but the results were still almost meaningless, particularly at the higher blowing rates. It was realised that this fluctuation along the plate was caused by the small scatter in the measurements, since this scatter is magnified by the differentiation. This scatter is partly due to the experimental accuracy; however, a more important cause may be the unavoidable variations in injection rate along the plate. The effect of this scatter is best seen by noting that equation (6) reduces to the momentum integral equation (equation (1)) in the outer part of the layer. From this equation it is easy to see that if $d\theta/dx$ is found directly from the measured values of θ by numerical differentiation then C_f is likely to vary in a random manner along the plate. For example, if we evaluate $d\theta/dx$ by the formula

$$\left(\frac{d\theta}{dx}\right)_{\text{Station } n} = \frac{\theta_{n+2} - \theta_{n-2}}{2}$$

(since $dx = 2$ inches in this case) then an error of $\pm 0{\cdot}0001$ in θ can give a maximum error of $0{\cdot}0002$ in C_f. In fact the possible errors in θ are probably greater than $0{\cdot}0001$, especially at the higher blowing rates. Thus it is apparent that the sheer-stress profiles calculated from equation (6) will be subject to large random errors.

However, Figs. 10, 11 and 12 show that the velocity profiles are similar over the front part of the plates, and so shear-stress profiles can be found from these similar profiles. In this case the shear stress is given by

$$\frac{\tau}{\rho_1 U_1^2} = F(f(\eta) - 1) + \frac{d\theta}{dx}\left[1 - f(\eta)\int_0^\eta f(\eta')\,g(\eta')\,d\eta' + \int_0^\eta f^2(\eta')\,g(\eta')\,d\eta'\right] \tag{7}$$

where $\eta = y/\theta$, $f = u/U_1$, and $g = \rho/\rho_1$. It should be noted that the pressure-gradient term has been ignored in equation (7) since its effect was found to be very small. Using values of $f(\eta)$ from Figs. 10, 11 and 12, and least-squares values of $d\theta/dx$ shear stress profiles were found for all the Mach numbers and blowing rates. The results are plotted in Figs. 17, 18 and 19. The corresponding values of eddy viscosity (i.e. $\tau/(du/dy)$) are plotted in Fig. 20.

Although the actual values of shear stress may be subject to error it is believed that the main features illustrated in Figs. 17, 18 and 19 are qualitatively correct. In particular it is of interest to note that the position of the maximum shear stress moves out with increasing Mach number. The results for eddy viscosity inevitably show a large amount of scatter. However, Fig. 20 shows that the ratio of eddy viscosity to (laminar viscosity $\times R_\theta$) is almost independent of injection and Mach number.

5. *Conclusions.*

Additional measurements have been made in the compressible turbulent boundary layer with air injection at Mach numbers of 1·8 and 2·5.

The results, together with results for incompressible flow, and for higher supersonic speeds, have been used to derive a universal velocity defect law. Shear-stress profiles have been obtained from the velocity profiles, and it has been found that the corresponding eddy viscosity distribution could be collapsed into a form almost independent of Mach number and injection rate.

LIST OF SYMBOLS

C_f	Local skin-friction coefficient
F	Injection parameter $= \rho_w v_w / \rho_1 U_1$
H	Boundary-layer shape parameter
M	Mach number
p	Static pressure
T	Static temperature
U_1	Free-stream velocity
u	Velocity in x-direction
U_τ	Frictional velocity
U_*	Modified frictional velocity (equation 4)
v	Velocity normal to the wall (y-direction)
x	Co-ordinate along the wall
y	Co-ordinate normal to the wall
δ	Boundary-layer thickness
θ	Momentum thickness
ρ	Density
τ	Shear stress

Subscripts

r	Recovery condition
w	Wall condition
1	Free-stream condition

REFERENCES

No.	*Author(s)*	*Title, etc.*
1	L. O. F. Jeromin	An experimental investigation of the compressible turbulent boundary layer with air injection. A.R.C. R. & M. 3526 (1966).
2	J. McQuaid	Experiments on incompressible turbulent boundary layers with distributed injection. A.R.C. R. & M. 3549 (1967).
3	L. C. Squire	A law of the wall for compressible turbulent boundary layers with air injection *J. Fluid Mech.* Vol. 37, pp. 449–456 (1969).
4	D. E. Coles	Measurements in the turbulent boundary layer on a smooth flat plate in supersonic flow. Jet Propulsion Laboratory; C.I.T. Report 20–71 (1953).
5	W. H. Schutts, W. H. Harting .. and J. R. Weiler	Turbulent boundary layer and skin-friction measurements on a smooth thermally insulated flat plate in supersonic flow. Univ. of Texas Defence Research Lab. DRL–364; CM823 (1955).
6	C. J. Stalmach	Experimental investigations of the surface impact probe method of measuring local skin friction at supersonic speeds. Univ. of Texas Defence Research Lab. DRL–410; CF–2675 (1958).
7	J. McQuaid	A velocity defect relationship for the outer part of equilibrium and near-equilibrium turbulent boundary layers. A.R.C. CP 885 (1965).

TABLE 1

NOMINAL MACH NUMBER= 1.80
INJECTION PARAMETER= 0.0000

Y	U/U1 (1)	U/U1 (3)	U/U1 (5)	U/U1 (7)	U/U1 (9)	U/U1 (11)
0.0032	0.506	0.514	0.503	0.502	0.498	0.492
0.0050	0.555	0.541	0.545	0.542	0.536	0.540
0.0100	0.640	0.619	0.623	0.620	0.608	0.618
0.0150	0.680	0.676	0.666	0.666	0.648	0.652
0.0200	0.714	0.700	0.699	0.695	0.682	0.687
0.0250	0.749	0.726	0.724	0.722	0.710	0.711
0.0300	0.772	0.748	0.743	0.738	0.732	0.728
0.0350	0.783	0.767	0.762	0.756	0.750	0.743
0.0400	0.800	0.782	0.776	0.774	0.764	0.757
0.0450	0.817	0.799	0.789	0.788	0.778	0.769
0.0500	0.832	0.815	0.804	0.799	0.793	0.781
0.0550	0.846	0.831	0.817	0.810	0.806	0.794
0.0600	0.861	0.845	0.829	0.824	0.818	0.804
0.0650	0.875	0.857	0.841	0.837	0.829	0.815
0.0700	0.887	0.869	0.855	0.847	0.841	0.825
0.0800	0.910	0.890	0.877	0.866	0.857	0.847
0.0900	0.932	0.911	0.897	0.886	0.876	0.865
0.1000	0.951	0.932	0.915	0.904	0.893	0.880
0.1100	0.967	0.950	0.933	0.923	0.910	0.897
0.1200	0.979	0.965	0.952	0.939	0.927	0.914
0.1300	0.986	0.978	0.964	0.954	0.944	0.930
0.1400	0.992	0.986	0.975	0.967	0.958	0.944
0.1500	0.995	0.993	0.985	0.978	0.969	0.957
0.1600	0.996	0.996	0.991	0.986	0.980	0.969
0.1700	0.997	0.998	0.995	0.992	0.987	0.979
0.1800	0.999	0.999	0.997	0.995	0.992	0.986
0.1900	0.999	0.999	0.998	0.997	0.997	0.992
0.2000	0.999	0.999	0.999	0.998	0.998	0.996
0.2100	1.000	1.000	0.999	0.999	0.999	0.997
0.2200	1.000	1.000	0.999	0.999	0.999	0.998
0.2300	1.000	1.000	1.000	0.999	0.999	0.999
0.2400	1.000	1.000	1.000	0.999	0.999	0.999
0.2500	1.000	1.000	1.000	0.999	1.000	0.999
0.2600	1.000	1.000	1.000	1.000	1.000	1.000
THETA	0.0121	0.0134	0.0146	0.0154	0.0163	0.0175
DELTA STAR	0.0350	0.0386	0.0417	0.0441	0.0465	0.0496

TABLE 2

NOMINAL MACH NUMBER= 1.80
INJECTION PARAMETER= 0.0013

Y	U/U1 (1)	U/U1 (3)	U/U1 (5)	U/U1 (7)	U/U1 (9)	U/U1 (11)
0.0032	0.406	0.412	0.398	0.405	0.391	0.395
0.0060	0.446	0.453	0.457	0.462	0.449	0.452
0.0120	0.516	0.520	0.532	0.536	0.520	0.528
0.0180	0.566	0.566	0.565	0.570	0.554	0.566
0.0240	0.600	0.596	0.588	0.593	0.583	0.592
0.0300	0.628	0.623	0.615	0.612	0.601	0.611
0.0360	0.654	0.645	0.636	0.632	0.620	0.628
0.0420	0.675	0.664	0.652	0.650	0.640	0.643
0.0480	0.695	0.682	0.668	0.667	0.654	0.660
0.0540	0.713	0.699	0.687	0.684	0.669	0.675
0.0600	0.732	0.715	0.703	0.699	0.683	0.686
0.0700	0.761	0.745	0.725	0.721	0.706	0.706
0.080	0.788	0.770	0.748	0.742	0.726	0.724
0.0900	0.815	0.794	0.770	0.761	0.745	0.741
0.1000	0.839	0.820	0.794	0.783	0.764	0.760
0.1150	0.876	0.855	0.827	0.815	0.795	0.787
0.1300	0.913	0.885	0.857	0.844	0.826	0.814
0.1450	0.940	0.917	0.888	0.872	0.851	0.839
0.1600	0.965	0.944	0.915	0.897	0.875	0.863
0.1750	0.983	0.963	0.939	0.921	0.900	0.883
0.1900	0.992	0.981	0.959	0.942	0.921	0.904
0.2050	0.997	0.991	0.976	0.960	0.940	0.923
0.2200	0.998	0.997	0.988	0.976	0.959	0.942
0.2350	0.999	0.999	0.994	0.986	0.975	0.958
0.2500	1.000	0.999	0.998	0.993	0.985	0.970
0.2650	1.000	1.000	0.999	0.996	0.991	0.980
0.2800	1.000	1.000	0.999	0.998	0.994	0.987
0.2950	1.000	1.000	1.000	0.999	0.996	0.992
0.3100	1.000	1.000	1.000	0.999	0.998	0.996
0.3250	1.000	1.000	1.000	0.999	0.999	0.997
0.3400	1.000	1.000	1.000	1.000	1.000	0.999
0.3550	1.000	1.000	1.000	1.000	1.000	0.999
0.3700	1.000	1.000	1.000	1.000	1.000	1.000
THETA	0.0200	0.0218	0.0244	0.0260	0.0284	0.0302
DELTA STAR	0.0606	0.0657	0.0724	0.0769	0.0830	0.0877

TABLE 3

NOMINAL MACH NUMBER= 1.80
INJECTION PARAMETER= 0.0025

Y	U/U1 (1)	U/U1 (3)	U/U1 (5)	U/U1 (7)	U/U1 (9)	U/U1 (11)
0.0032	0.336	0.322	0.315	0.333	0.326	0.304
0.0070	0.395	0.358	0.377	0.387	0.399	0.383
0.0140	0.482	0.424	0.446	0.455	0.448	0.445
0.0210	0.493	0.473	0.479	0.491	0.485	0.481
0.0280	0.522	0.508	0.512	0.511	0.511	0.506
0.0350	0.548	0.534	0.535	0.534	0.530	0.528
0.0420	0.572	0.558	0.552	0.554	0.551	0.550
0.0490	0.596	0.578	0.573	0.573	0.567	0.562
0.0560	0.620	0.597	0.594	0.589	0.583	0.574
0.0630	0.637	0.617	0.612	0.605	0.599	0.588
0.0700	0.655	0.636	0.629	0.620	0.611	0.602
0.0850	0.694	0.670	0.657	0.651	0.639	0.630
0.1000	0.736	0.713	0.695	0.679	0.668	0.655
0.1150	0.780	0.750	0.724	0.708	0.697	0.683
0.1300	0.816	0.784	0.756	0.737	0.723	0.709
0.1450	0.851	0.816	0.789	0.767	0.749	0.734
0.1600	0.885	0.847	0.813	0.795	0.773	0.761
0.1750	0.917	0.877	0.847	0.824	0.803	0.786
0.1900	0.945	0.905	0.871	0.850	0.826	0.806
0.2050	0.966	0.931	0.898	0.873	0.851	0.826
0.2200	0.981	0.954	0.924	0.899	0.874	0.847
0.2350	0.991	0.972	0.947	0.920	0.896	0.869
0.2500	0.996	0.985	0.963	0.941	0.919	0.890
0.2650	0.998	0.992	0.976	0.959	0.937	0.909
0.2800	0.999	0.995	0.986	0.974	0.953	0.926
0.2950	1.000	0.998	0.992	0.984	0.967	0.944
0.3100	1.000	0.999	0.995	0.991	0.979	0.959
0.3250	1.000	1.000	0.997	0.996	0.988	0.972
0.3400	1.000	1.000	0.999	0.999	0.993	0.982
0.3550	1.000	1.000	0.999	0.999	0.997	0.989
0.3700	1.000	1.000	0.999	1.000	0.998	0.994
0.3850	1.000	1.000	1.000	1.000	0.999	0.997
0.4000	1.000	1.000	1.000	1.000	1.000	0.999
THETA	0.0268	0.0300	0.0333	0.0357	0.0386	0.0418
DELTA STAR	0.0858	0.0960	0.1044	0.1115	0.1184	0.1274

TABLE 4

NOMINAL MACH NUMBER= 1.80
INJECTION PARAMETER= 0.0031

Y	U/U1 (1)	U/U1 (3)	U/U1 (5)	U/U1 (7)	U/U1 (9)	U/U1 (11)
0.0032	0.262	0.261	0.262	0.247	0.290	0.289
0.0100	0.352	0.348	0.383	0.352	0.387	0.367
0.0200	0.434	0.418	0.428	0.419	0.440	0.427
0.0300	0.471	0.464	0.472	0.468	0.474	0.473
0.0400	0.511	0.502	0.499	0.496	0.500	0.505
0.0500	0.541	0.532	0.530	0.521	0.523	0.526
0.0600	0.570	0.561	0.558	0.543	0.546	0.543
0.0700	0.598	0.585	0.583	0.565	0.567	0.560
0.0800	0.625	0.609	0.604	0.584	0.585	0.580
0.1000	0.677	0.656	0.647	0.623	0.617	0.614
0.1200	0.735	0.704	0.689	0.665	0.659	0.647
0.1400	0.784	0.749	0.732	0.708	0.694	0.678
0.1600	0.835	0.793	0.770	0.746	0.727	0.707
0.1800	0.876	0.835	0.809	0.780	0.759	0.739
0.2000	0.918	0.876	0.846	0.815	0.792	0.769
0.2200	0.952	0.915	0.880	0.848	0.824	0.799
0.2400	0.976	0.945	0.915	0.879	0.855	0.831
0.2600	0.990	0.968	0.943	0.911	0.884	0.858
0.2800	0.996	0.984	0.965	0.937	0.910	0.886
0.3000	0.999	0.993	0.981	0.960	0.938	0.910
0.3200	1.000	0.997	0.989	0.977	0.959	0.933
0.3400	1.000	0.999	0.995	0.988	0.976	0.954
0.3600	1.000	1.000	0.998	0.994	0.986	0.970
0.3800	1.000	1.000	1.000	0.997	0.993	0.984
0.4000	1.000	1.000	1.000	0.999	0.997	0.992
0.4200	1.000	1.000	1.000	1.000	0.999	0.997
0.4400	1.000	1.000	1.000	1.000	1.000	0.999
THETA	0.0306	0.0343	0.0374	0.0410	0.0440	0.0474
DELTA STAR	0.1021	0.1129	0.1211	0.1317	0.1394	0.1481

TABLE 5

NOMINAL MACH NUMBER= 2.50
INJECTION PARAMETER= 0.0000

Y	U/U1 (1)	U/U1 (3)	U/U1 (5)	U/U1 (7)	U/U1 (9)	U/U1 (11)
0.0032	0.474	0.460	0.467	0.448	0.474	0.460
0.0050	0.504	0.501	0.507	0.485	0.515	0.501
0.0100	0.577	0.583	0.589	0.571	0.594	0.583
0.0150	0.634	0.630	0.639	0.635	0.638	0.634
0.0200	0.674	0.662	0.670	0.678	0.667	0.665
0.0250	0.699	0.691	0.695	0.697	0.693	0.688
0.0300	0.723	0.715	0.714	0.713	0.713	0.708
0.0350	0.744	0.730	0.732	0.730	0.727	0.723
0.0400	0.762	0.745	0.748	0.744	0.741	0.737
0.0450	0.778	0.760	0.759	0.757	0.755	0.748
0.0500	0.792	0.775	0.772	0.770	0.768	0.760
0.0550	0.807	0.789	0.785	0.780	0.779	0.770
0.0600	0.819	0.803	0.798	0.790	0.789	0.781
0.0650	0.831	0.814	0.810	0.800	0.799	0.791
0.0700	0.843	0.826	0.821	0.809	0.808	0.801
0.0800	0.864	0.848	0.842	0.829	0.827	0.819
0.0900	0.886	0.870	0.862	0.849	0.848	0.836
0.1000	0.909	0.892	0.882	0.869	0.866	0.855
0.1100	0.927	0.909	0.904	0.886	0.881	0.872
0.1200	0.944	0.926	0.922	0.902	0.898	0.888
0.1300	0.959	0.944	0.937	0.919	0.917	0.903
0.1400	0.972	0.958	0.950	0.934	0.933	0.916
0.1500	0.984	0.971	0.964	0.948	0.943	0.928
0.1600	0.993	0.982	0.974	0.961	0.954	0.941
0.1700	0.995	0.989	0.984	0.971	0.965	0.954
0.1800	0.997	0.993	0.991	0.981	0.976	0.966
0.1900	0.998	0.997	0.995	0.988	0.984	0.976
0.2000	0.999	0.998	0.998	0.992	0.991	0.984
0.2100	0.999	0.999	0.999	0.996	0.996	0.990
0.2200	1.000	0.999	0.999	0.997	0.998	0.994
0.2300	1.000	0.999	1.000	0.998	0.999	0.997
0.2400	1.000	1.000	1.000	0.999	0.999	0.998
0.2500	1.000	1.000	1.000	0.999	0.999	0.999
0.2600	1.000	1.000	1.000	1.000	1.000	0.999
THETA	0.0130	0.0143	0.0148	0.0160	0.0163	0.0174
DELTA STAR	0.0549	0.0596	0.0613	0.0667	0.0678	0.0722

TABLE 6

NOMINAL MACH NUMBER= 2.50
INJECTION PARAMETER= 0.0013

Y	U/U1 (1)	U/U1 (3)	U/U1 (5)	U/U1 (7)	U/U1 (9)	U/U1 (11)
0.0032	0.365	0.341	0.377	0.369	0.339	0.358
0.0060	0.401	0.398	0.473	0.473	0.406	0.417
0.0120	0.451	0.463	0.481	0.486	0.453	0.485
0.0180	0.495	0.496	0.521	0.534	0.485	0.517
0.0240	0.541	0.538	0.552	0.569	0.527	0.541
0.0300	0.571	0.567	0.573	0.595	0.557	0.560
0.0360	0.596	0.587	0.591	0.617	0.579	0.580
0.0420	0.614	0.603	0.608	0.632	0.594	0.594
0.0480	0.633	0.624	0.621	0.644	0.609	0.610
0.0540	0.656	0.644	0.638	0.658	0.621	0.623
0.0600	0.677	0.663	0.657	0.671	0.637	0.636
0.0700	0.706	0.689	0.683	0.693	0.663	0.660
0.0800	0.730	0.711	0.700	0.715	0.687	0.680
0.0900	0.758	0.734	0.721	0.731	0.704	0.697
0.1000	0.784	0.759	0.745	0.749	0.721	0.717
0.1150	0.823	0.796	0.780	0.780	0.747	0.745
0.1300	0.858	0.826	0.811	0.806	0.777	0.771
0.1450	0.888	0.857	0.841	0.832	0.804	0.793
0.1600	0.917	0.893	0.870	0.856	0.831	0.818
0.1750	0.943	0.915	0.895	0.880	0.855	0.843
0.1900	0.964	0.935	0.919	0.903	0.877	0.863
0.2050	0.982	0.958	0.940	0.922	0.897	0.887
0.2200	0.993	0.976	0.960	0.940	0.917	0.905
0.2350	0.998	0.988	0.978	0.958	0.937	0.922
0.2500	0.999	0.995	0.990	0.975	0.955	0.939
0.2650	0.999	0.998	0.996	0.986	0.970	0.956
0.2800	1.000	0.999	0.999	0.992	0.983	0.971
0.2950	1.000	1.000	0.999	0.996	0.991	0.983
0.3100	1.000	1.000	0.999	0.998	0.997	0.990
0.3250	1.000	1.000	1.000	1.000	0.998	0.994
0.3400	1.000	1.000	1.000	1.000	0.999	0.997
0.3550	1.000	1.000	1.000	1.000	1.000	0.998
0.3700	1.000	1.000	1.000	1.000	1.000	0.999
THETA	0.0202	0.0225	0.0240	0.0252	0.0278	0.0292
DELTA STAR	0.0904	0.0993	0.1048	0.1104	0.1210	0.1265

TABLE 7

NOMINAL MACH NUMBER= 2.50
INJECTION PARAMETER= 0.0024

Y	U/U1 (1)	U/U1 (3)	U/U1 (5)	U/U1 (7)	U/U1 (9)	U/U1 (11)
0.0032	0.264	0.201	0.284	0.279	0.267	0.299
0.0070	0.319	0.330	0.369	0.328	0.326	0.372
0.0140	0.385	0.305	0.408	0.396	0.372	0.395
0.0210	0.420	0.383	0.436	0.427	0.397	0.439
0.0280	0.446	0.422	0.467	0.460	0.427	0.464
0.0350	0.466	0.453	0.484	0.484	0.452	0.487
0.0420	0.490	0.477	0.502	0.500	0.467	0.506
0.0490	0.517	0.499	0.518	0.519	0.486	0.519
0.0560	0.540	0.517	0.535	0.533	0.503	0.531
0.0630	0.557	0.541	0.554	0.552	0.515	0.545
0.0700	0.571	0.565	0.570	0.565	0.531	0.558
0.0850	0.614	0.600	0.595	0.590	0.563	0.583
0.1000	0.650	0.631	0.626	0.620	0.590	0.606
0.1150	0.693	0.663	0.659	0.649	0.617	0.633
0.1300	0.733	0.699	0.685	0.674	0.646	0.659
0.1450	0.773	0.737	0.718	0.699	0.673	0.687
0.1600	0.810	0.769	0.747	0.728	0.698	0.710
0.1750	0.841	0.802	0.777	0.755	0.724	0.736
0.1900	0.873	0.831	0.805	0.780	0.746	0.757
0.2050	0.902	0.858	0.833	0.806	0.771	0.777
0.2200	0.930	0.889	0.860	0.833	0.796	0.801
0.2350	0.953	0.916	0.885	0.852	0.821	0.822
0.2500	0.973	0.941	0.909	0.878	0.855	0.848
0.2650	0.987	0.963	0.930	0.896	0.864	0.862
0.2800	0.995	0.980	0.949	0.916	0.885	0.881
0.2950	0.997	0.992	0.966	0.935	0.907	0.901
0.3100	0.998	0.996	0.981	0.952	0.926	0.919
0.3250	0.999	0.998	0.990	0.968	0.945	0.936
0.3400	0.999	0.999	0.995	0.978	0.960	0.950
0.3550	0.999	0.999	0.998	0.985	0.973	0.963
0.3700	1.000	0.999	0.999	0.992	0.983	0.974
0.3850	1.000	0.999	0.999	0.994	0.990	0.983
0.4000	1.000	1.000	1.000	0.995	0.994	0.990
0.4150	1.000	1.000	1.000	0.996	0.996	0.994
0.4300	1.000	1.000	1.000	0.998	0.998	0.996
0.4450	1.000	1.000	1.000	0.999	0.999	0.997
THETA	0.0269	0.0297	0.0326	0.0356	0.0387	0.0393
DELTA STAR	0.1285	0.1418	0.1517	0.1661	0.1793	0.1802

TABLE 8

NOMINAL MACH NUMBER= 2.50
INJECTION PARAMETER= 0.0036

Y	U/U1 (1)	U/U1 (3)	U/U1 (5)	U/U1 (7)	U/U1 (9)	U/U1 (11)
0.0032	0.220	0.139	0.252	0.220	0.243	0.290
0.0100	0.264	0.202	0.303	0.262	0.273	0.312
0.0200	0.301	0.264	0.350	0.294	0.317	0.339
0.0300	0.345	0.311	0.383	0.344	0.343	0.363
0.0400	0.378	0.346	0.410	0.379	0.358	0.382
0.0500	0.409	0.373	0.435	0.403	0.383	0.394
0.0600	0.431	0.402	0.456	0.424	0.408	0.405
0.0700	0.456	0.428	0.471	0.443	0.431	0.423
0.0800	0.481	0.452	0.488	0.461	0.444	0.444
0.1000	0.528	0.496	0.527	0.495	0.482	0.474
0.1200	0.580	0.537	0.557	0.533	0.515	0.504
0.1400	0.623	0.589	0.590	0.568	0.542	0.534
0.1600	0.673	0.631	0.628	0.601	0.576	0.562
0.1800	0.719	0.673	0.663	0.632	0.610	0.599
0.2000	0.767	0.718	0.697	0.664	0.641	0.627
0.2200	0.811	0.761	0.733	0.696	0.673	0.660
0.2400	0.856	0.801	0.774	0.732	0.703	0.694
0.2600	0.893	0.839	0.809	0.767	0.737	0.724
0.2800	0.930	0.879	0.841	0.798	0.766	0.750
0.3000	0.959	0.913	0.875	0.829	0.798	0.779
0.3200	0.982	0.945	0.903	0.862	0.825	0.807
0.3400	0.993	0.970	0.928	0.890	0.852	0.834
0.3600	0.997	0.987	0.953	0.914	0.876	0.860
0.3800	0.998	0.994	0.973	0.937	0.903	0.883
0.4000	0.999	0.998	0.987	0.958	0.925	0.906
0.4200	1.000	0.999	0.993	0.973	0.944	0.927
0.4400	1.000	1.000	0.997	0.985	0.962	0.939
0.4600	1.000	1.000	0.998	0.992	0.974	0.960
0.4800	1.000	1.000	0.999	0.996	0.983	0.976
0.5000	1.000	1.000	1.000	0.998	0.989	0.985
0.5200	1.000	1.000	1.000	0.999	0.994	0.991
0.5400	1.000	1.000	1.000	1.000	0.997	0.994
0.5600	1.000	1.000	1.000	1.000	1.000	0.997
0.5800	1.000	1.000	1.000	1.000	1.000	0.999
THETA	0.0340	0.0373	0.0417	0.0456	0.0502	0.0523
DELTA STAR	0.1742	0.1940	0.2063	0.2278	0.2456	0.2562

TABLE 9

NOMINAL MACH NUMBER= 3.60
INJECTION PARAMETER= 0.0000

Y	U/U1 (1)	U/U1 (3)	U/U1 (5)	U/U1 (7)	U/U1 (9)
0.0032	0.422	0.412	0.434	0.425	0.412
0.0050	0.519	0.498	0.493	0.497	0.459
0.0100	0.583	0.587	0.593	0.587	0.563
0.0150	0.635	0.634	0.636	0.634	0.613
0.0200	0.674	0.668	0.669	0.665	0.653
0.0250	0.698	0.690	0.690	0.689	0.677
0.0300	0.716	0.707	0.708	0.707	0.693
0.0350	0.732	0.721	0.721	0.720	0.706
0.0400	0.746	0.732	0.735	0.732	0.721
0.0450	0.759	0.744	0.747	0.744	0.734
0.0500	0.770	0.757	0.758	0.755	0.744
0.0550	0.781	0.769	0.768	0.765	0.753
0.0600	0.793	0.781	0.777	0.774	0.761
0.0650	0.805	0.792	0.788	0.785	0.772
0.0700	0.817	0.802	0.799	0.794	0.783
0.0800	0.839	0.824	0.819	0.814	0.801
0.0900	0.859	0.843	0.839	0.832	0.819
0.1000	0.877	0.861	0.856	0.850	0.836
0.1100	0.897	0.879	0.873	0.867	0.852
0.1200	0.912	0.896	0.889	0.883	0.869
0.1300	0.929	0.912	0.905	0.898	0.884
0.1400	0.943	0.931	0.920	0.912	0.898
0.1500	0.955	0.941	0.932	0.926	0.912
0.1600	0.968	0.954	0.945	0.939	0.925
0.1700	0.979	0.966	0.959	0.951	0.938
0.1800	0.987	0.977	0.970	0.962	0.950
0.1900	0.993	0.986	0.979	0.972	0.961
0.2000	0.997	0.993	0.987	0.982	0.971
0.2100	0.999	0.996	0.993	0.989	0.980
0.2200	1.000	0.998	0.997	0.994	0.988
0.2300	1.000	0.999	0.999	0.997	0.993
0.2400	1.000	1.000	0.999	0.999	0.996
0.2500	1.000	1.000	1.000	1.000	0.998
0.2600	1.000	1.000	1.000	1.000	0.999
THETA	0.0119	0.0129	0.0134	0.0140	0.0150
DELTA STAR	0.0828	0.0888	0.0920	0.0950	0.1012

TABLE 10

NOMINAL MACH NUMBER= 3.60
INJECTION PARAMETER= 0.00065

Y	U/U1 (1)	U/U1 (3)	U/U1 (5)	U/U1 (7)	U/U1 (9)
0.0032	0.365	0.362	0.366	0.379	0.379
0.0060	0.423	0.427	0.416	0.430	0.437
0.0120	0.483	0.485	0.485	0.491	0.503
0.0180	0.533	0.521	0.523	0.528	0.534
0.0240	0.571	0.560	0.555	0.562	0.565
0.0300	0.594	0.585	0.579	0.584	0.590
0.0360	0.620	0.608	0.598	0.605	0.609
0.0420	0.641	0.630	0.617	0.621	0.626
0.0480	0.659	0.646	0.635	0.637	0.641
0.0540	0.677	0.661	0.651	0.653	0.653
0.0600	0.693	0.676	0.666	0.665	0.664
0.0700	0.722	0.701	0.689	0.685	0.685
0.0800	0.746	0.722	0.712	0.706	0.706
0.0900	0.771	0.745	0.736	0.726	0.725
0.1000	0.793	0.768	0.756	0.746	0.743
0.1150	0.826	0.800	0.786	0.773	0.770
0.1300	0.854	0.829	0.815	0.801	0.796
0.1450	0.883	0.856	0.842	0.826	0.819
0.1600	0.908	0.881	0.867	0.851	0.844
0.1750	0.932	0.906	0.892	0.873	0.865
0.1900	0.954	0.930	0.915	0.896	0.886
0.2050	0.973	0.951	0.937	0.918	0.908
0.2200	0.987	0.969	0.957	0.938	0.928
0.2350	0.995	0.984	0.975	0.957	0.946
0.2500	0.998	0.993	0.988	0.974	0.964
0.2650	0.999	0.997	0.995	0.987	0.978
0.2800	1.000	0.998	0.998	0.994	0.988
0.2950	1.000	0.999	0.999	0.998	0.995
0.3100	1.000	1.000	1.000	0.999	0.998
0.3250	1.000	1.000	1.000	1.000	0.999
THETA	0.0157	0.0174	0.0183	0.0197	0.0204
DELTA STAR	0.1140	0.1247	0.1307	0.1379	0.1433

TABLE 11

NOMINAL MACH NUMBER= 3.60
INJECTION PARAMETER= 0.0012

Y	U/U1 (1)	U/U1 (3)	U/U1 (5)	U/U1 (7)	U/U1 (9)
0.0032	0.334	0.299	0.321	0.315	0.325
0.0070	0.396	0.363	0.370	0.362	0.377
0.0140	0.450	0.419	0.429	0.427	0.438
0.0210	0.485	0.464	0.466	0.465	0.471
0.0280	0.517	0.495	0.495	0.484	0.500
0.0350	0.542	0.521	0.521	0.509	0.520
0.0420	0.564	0.543	0.541	0.529	0.543
0.0490	0.584	0.562	0.554	0.546	0.559
0.0560	0.606	0.582	0.574	0.563	0.571
0.0630	0.626	0.600	0.592	0.578	0.585
0.0700	0.645	0.617	0.609	0.594	0.597
0.0850	0.685	0.654	0.645	0.625	0.630
0.1000	0.723	0.690	0.677	0.655	0.658
0.1150	0.757	0.725	0.708	0.688	0.686
0.1300	0.789	0.757	0.740	0.716	0.712
0.1450	0.820	0.786	0.769	0.743	0.737
0.1600	0.851	0.815	0.798	0.772	0.763
0.1750	0.879	0.844	0.824	0.798	0.787
0.1900	0.903	0.872	0.852	0.824	0.812
0.2050	0.928	0.896	0.877	0.849	0.834
0.2200	0.946	0.921	0.900	0.871	0.857
0.2350	0.966	0.943	0.922	0.894	0.876
0.2500	0.985	0.963	0.944	0.915	0.899
0.2650	0.994	0.979	0.963	0.937	0.918
0.2800	0.998	0.990	0.979	0.955	0.937
0.2950	0.999	0.996	0.990	0.971	0.953
0.3100	1.000	0.998	0.996	0.984	0.969
0.3250	1.000	0.999	0.998	0.992	0.982
0.3400	1.000	0.999	0.999	0.997	0.990
0.3550	1.000	1.000	1.000	0.999	0.995
0.3700	1.000	1.000	1.000	0.999	0.997
0.3850	1.000	1.000	1.000	1.000	0.999
0.4000	1.000	1.000	1.000	1.000	0.999
THETA	0.0188	0.0207	0.0219	0.0240	0.0254
DELTA STAR	00.1396	0.1533	0.1622	0.1754	0.1839

TABLE 12

NOMINAL MACH NUMBER= 3.60
INJECTION PARAMETER= 0.0021

Y	U/U1 (1)	U/U1 (3)	U/U1 (5)	U/U1 (7)	U/U1 (9)
0.0032	0.283	0.270	0.256	0.323	0.377
0.0100	0.320	0.318	0.307	0.348	0.393
0.0200	0.357	0.339	0.343	0.369	0.405
0.0300	0.388	0.376	0.369	0.383	0.428
0.0400	0.415	0.404	0.388	0.403	0.443
0.0500	0.445	0.428	0.414	0.427	0.461
0.0600	0.465	0.451	0.438	0.447	0.479
0.0700	0.493	0.478	0.458	0.462	0.495
0.0800	0.511	0.497	0.479	0.477	0.513
0.1000	0.559	0.536	0.518	0.514	0.545
0.1200	0.606	0.580	0.556	0.551	0.578
0.1400	0.652	0.624	0.592	0.580	0.616
0.1600	0.700	0.666	0.631	0.622	0.650
0.1800	0.745	0.709	0.670	0.662	0.687
0.2000	0.791	0.751	0.710	0.698	0.721
0.2200	0.834	0.792	0.751	0.732	0.752
0.2400	0.870	0.829	0.788	0.768	0.784
0.2600	0.906	0.864	0.823	0.802	0.813
0.2800	0.938	0.897	0.856	0.833	0.842
0.3000	0.965	0.928	0.888	0.863	0.870
0.3200	0.985	0.956	0.917	0.892	0.898
0.3400	0.995	0.979	0.945	0.920	0.922
0.3600	0.997	0.992	0.969	0.945	0.945
0.3800	0.998	0.998	0.985	0.996	0.965
0.4000	0.999	0.999	0.994	0.983	0.979
0.4200	0.999	1.000	0.998	0.992	0.990
0.4400	1.000	1.000	0.999	0.996	0.995
0.4600	1.000	1.000	1.000	0.998	0.998
0.4800	1.000	1.000	1.000	0.999	0.999
0.5000	1.000	1.000	1.000	1.000	0.999
THETA	0.0247	0.0271	0.0294	0.0317	0.0321
DELTA STAR	0.1969	0.2148	0.2361	0.2443	0.2421

TABLE 13

Skin-Friction Coefficients from Momentum.

$M = 1{\cdot}8$

F	C_f	
0	0·00203	(0·00208)
0·0013	0·00140	(0·00152)
0·0025	0·00050	(0·00090)
0·0031	0·00006	(0·00046)

$M = 2{\cdot}5$ (Squire, Low Reynolds number)

F	C_f	
0	0·00167	(0·00166)
0·0013	0·00100	(0·00104)
0·0024	0·00048	(0·00054)
0·0036	0·00052	(0·00060)

$M = 2{\cdot}5$ (Jeromin, High Reynolds number)

F	C_f
0	0·00160
0·0006	0·00115
0·0009	0·00097
0·0013	0·00072

$M = 3{\cdot}6$ (Jeromin)

F	C_f		C_f 'Corrected'
0	0·00138	(0·00128)	0·00118
0·00065	0·00099	(0·00089)	0·00079
0·0012	0·00076	(0·00065)	0·00056
0·0021	0·00057	(0·00048)	0·00037

N.B. Values in brackets show the value of C_f obtained by ignoring the pressure gradient term in equation (1). The 'corrected' results at $M = 3{\cdot}6$ are 0·0002 lower than the measured values because of possible three-dimensional effects.

In general the accuracy is $\pm 0{\cdot}0001$ at $F = 0$, and may be as high as $\pm 0{\cdot}00025$ at the highest blowing rate.

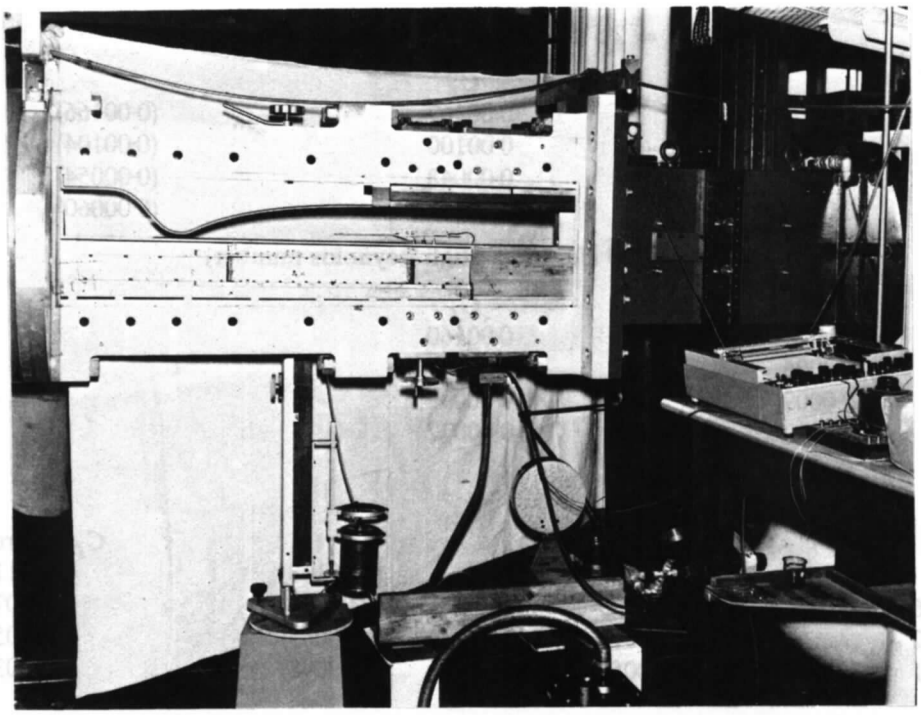

FIG. 1. Photograph of working section.

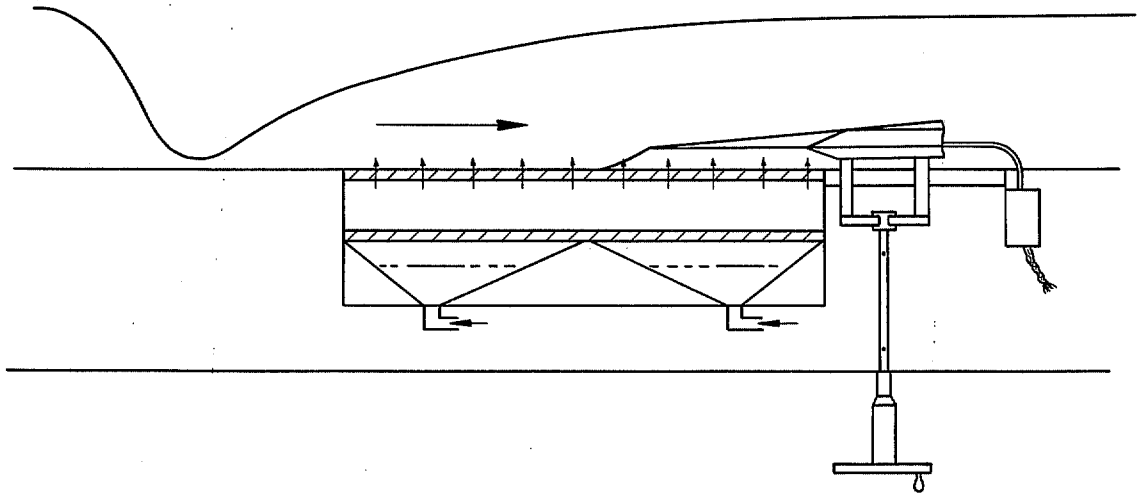

FIG. 2. Sketch of injection equipment.

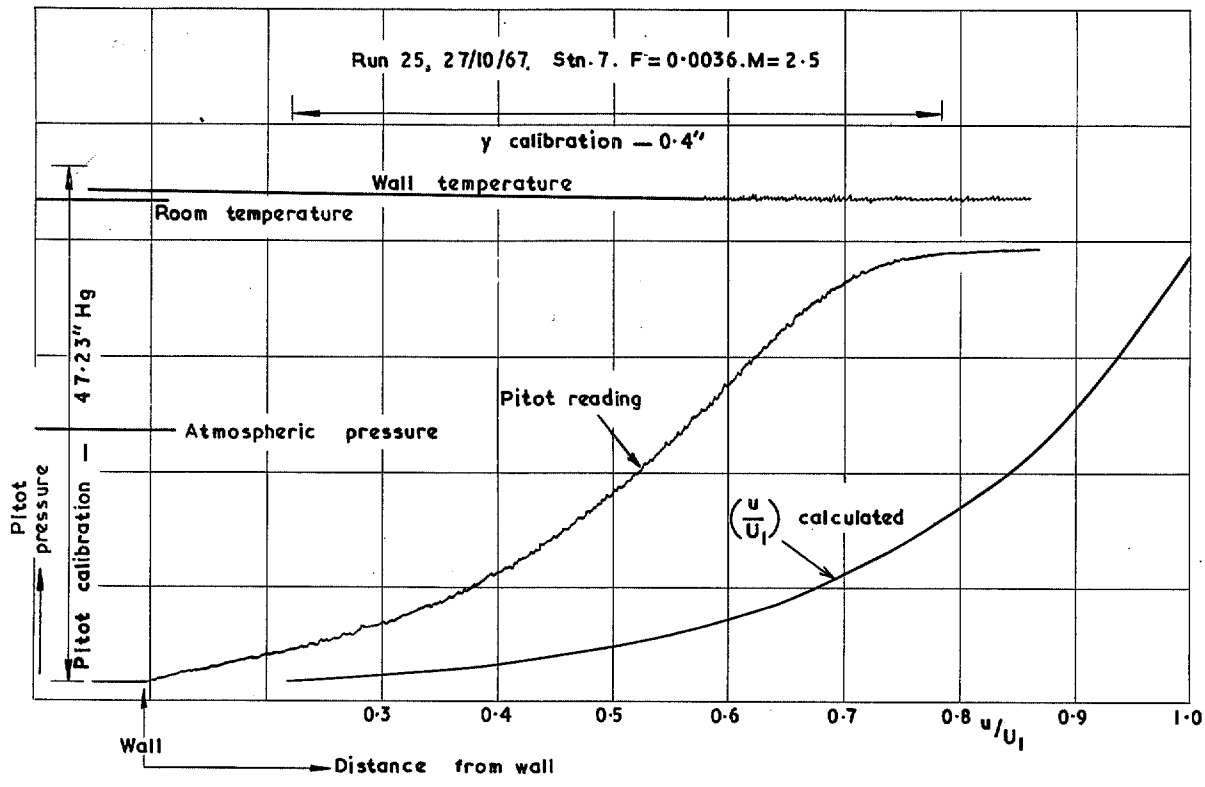

FIG. 3. Typical X-Y chart.

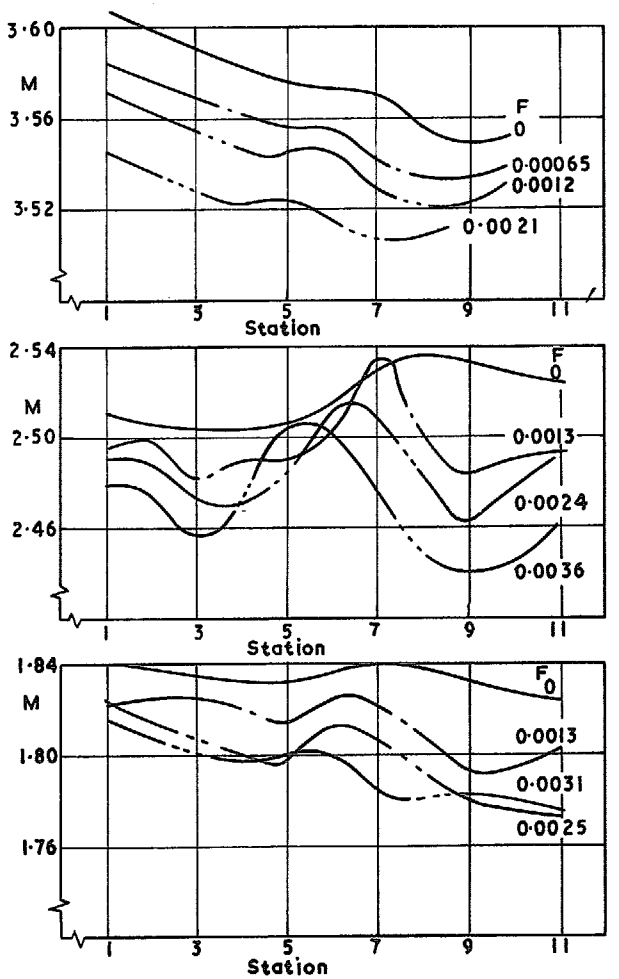

FIG. 4. Mach-number distributions.

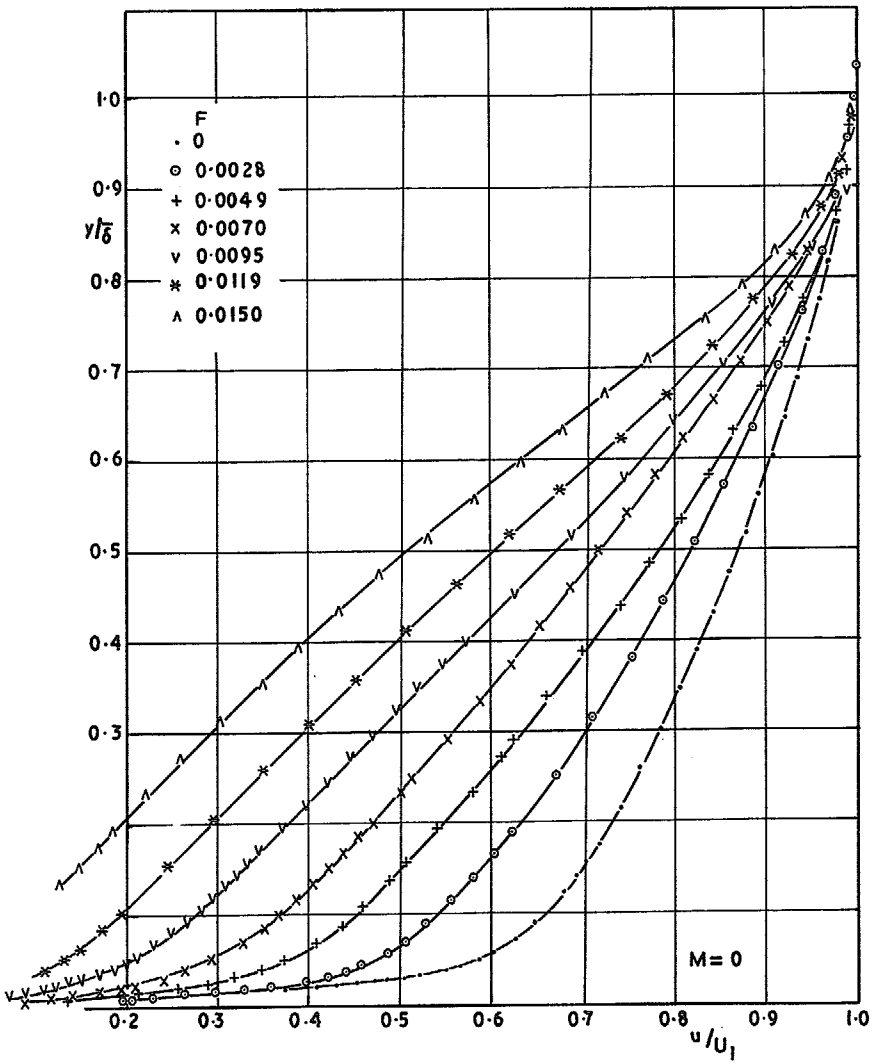

FIG. 5. Velocity profiles—$M = 0$.

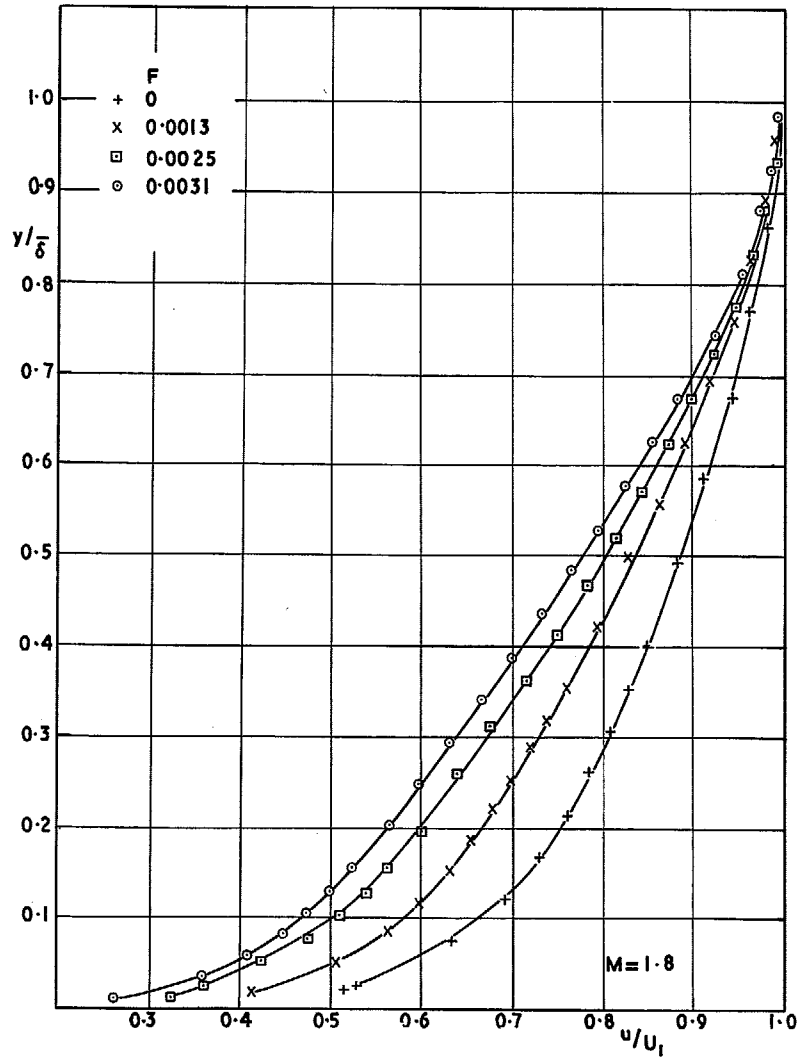

FIG. 6. Velocity profiles—$M = 1{\cdot}8$.

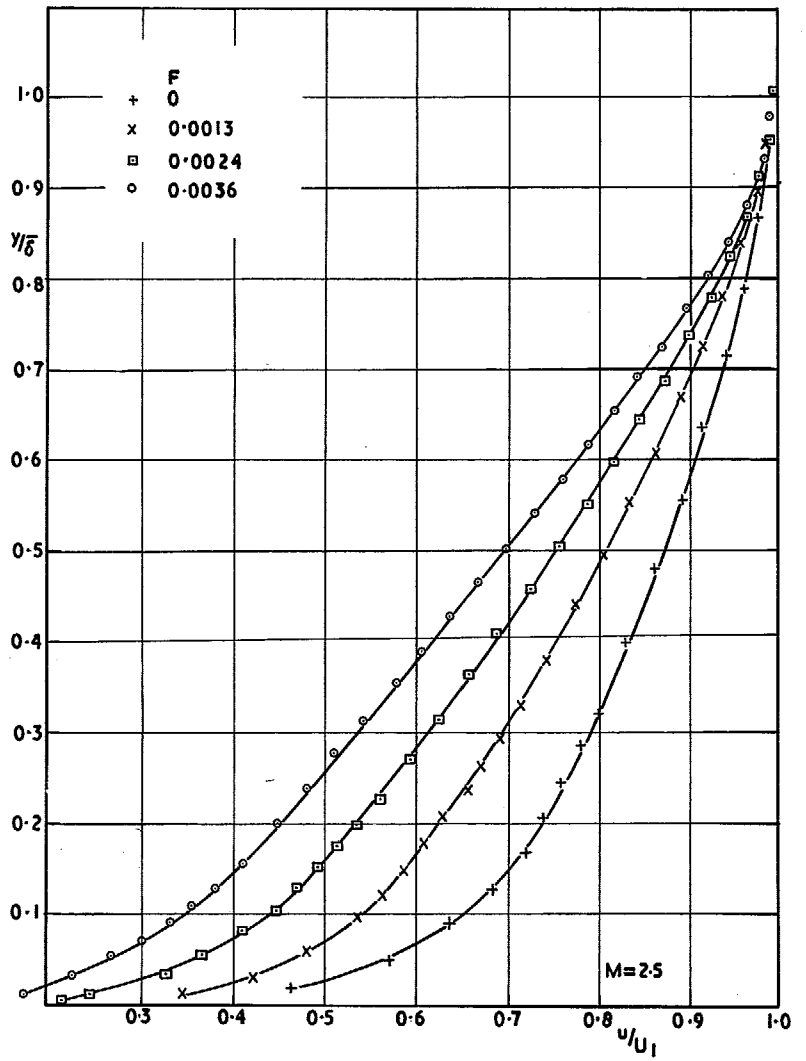

FIG. 7. Velocity profiles—$M = 2{\cdot}5$.

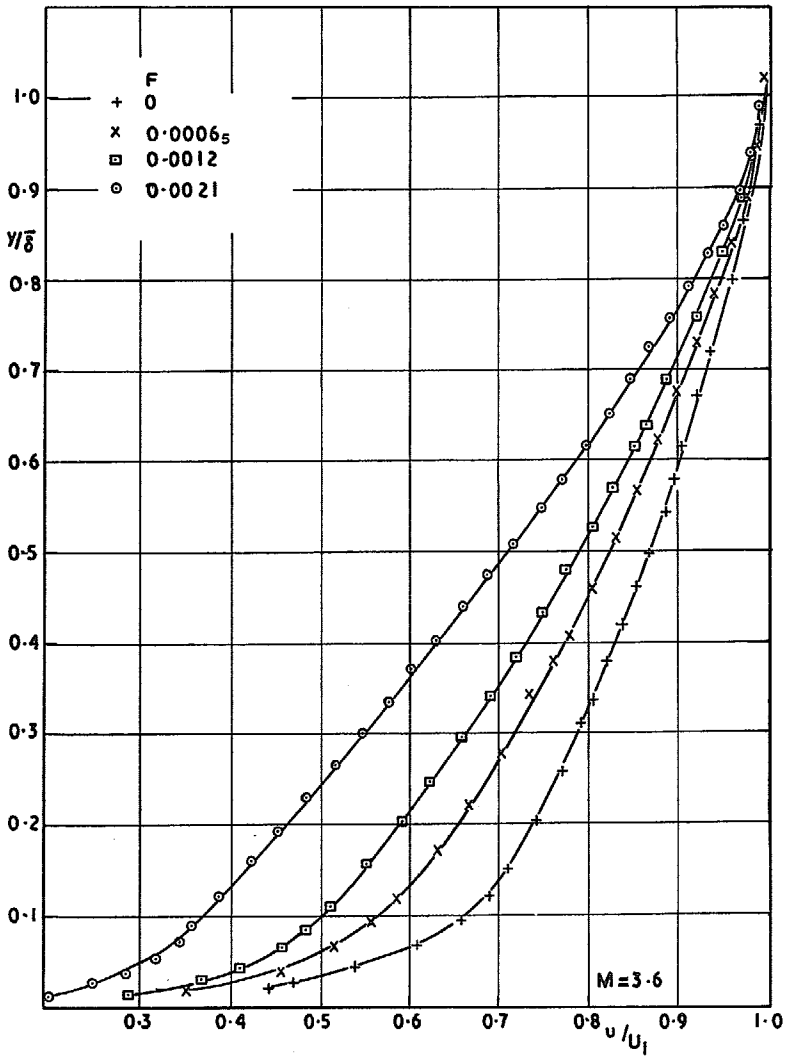

FIG. 8. Velocity profiles—$M = 3{\cdot}6$.

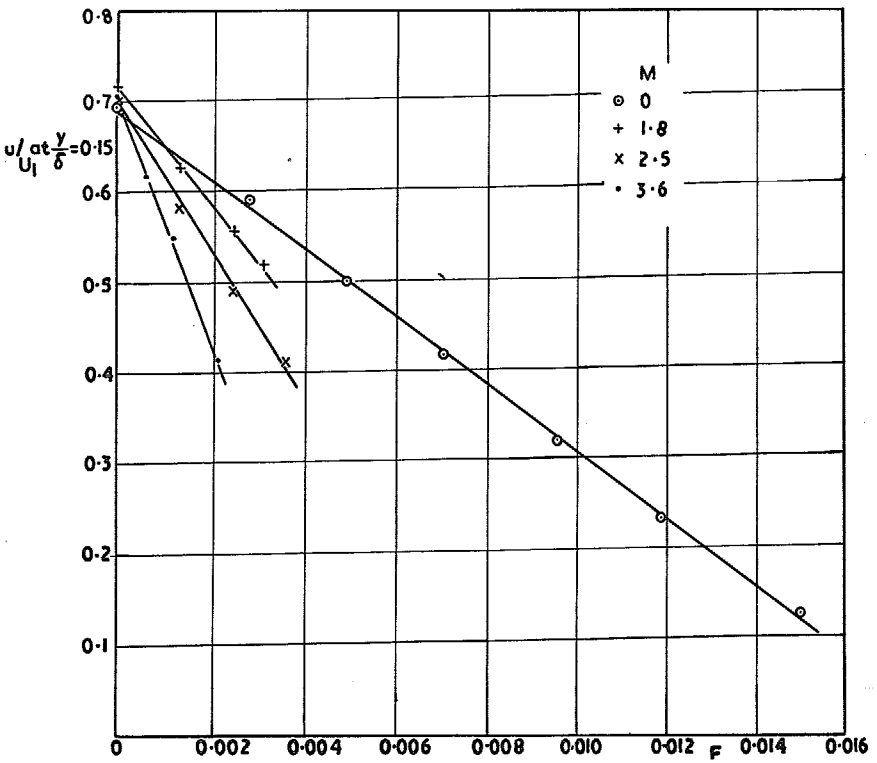

FIG. 9. Velocity ratios at $y/\delta = 0{\cdot}15$.

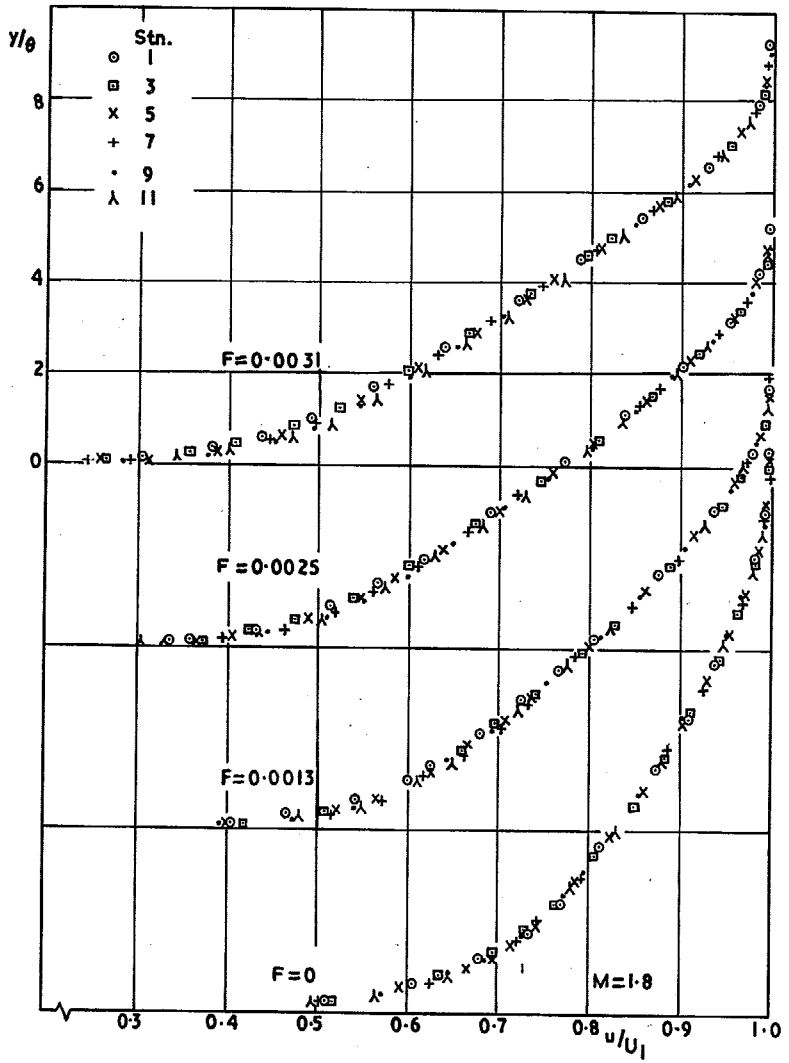

FIG. 10. Velocity profiles at $M = 1{\cdot}8$.

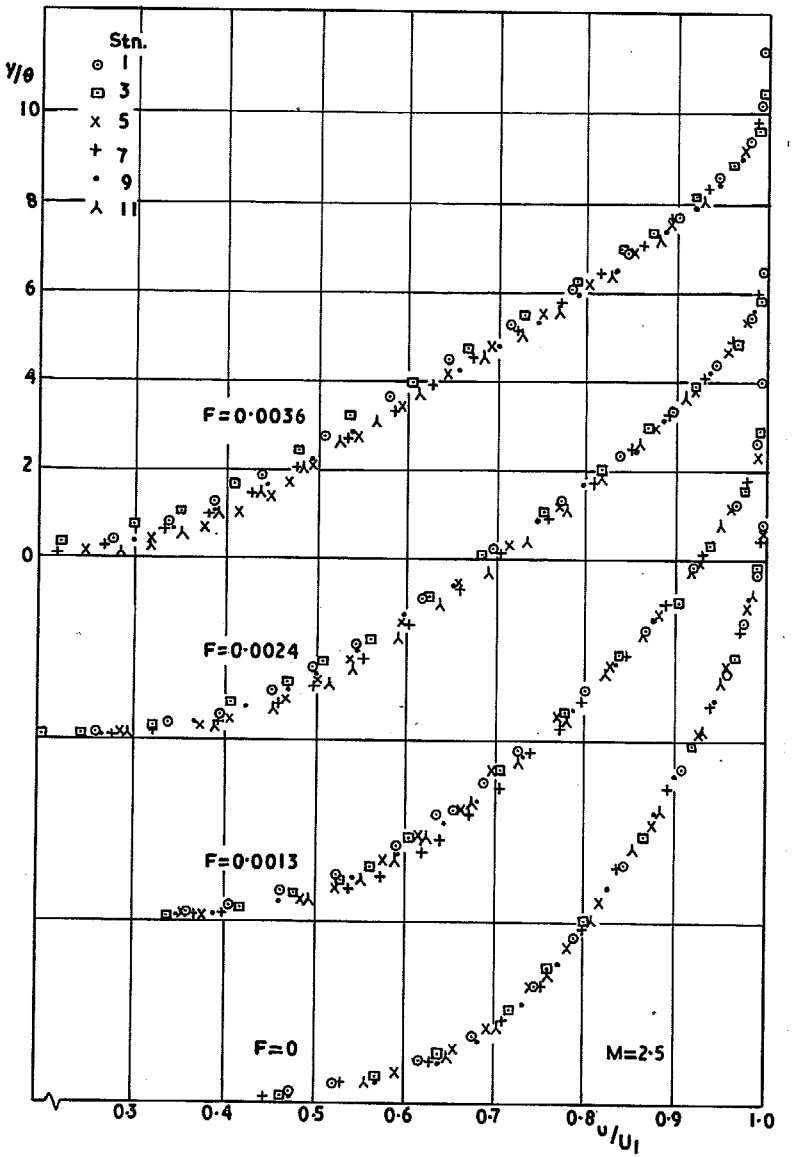

FIG. 11. Velocity profiles at $M = 2{\cdot}5$.

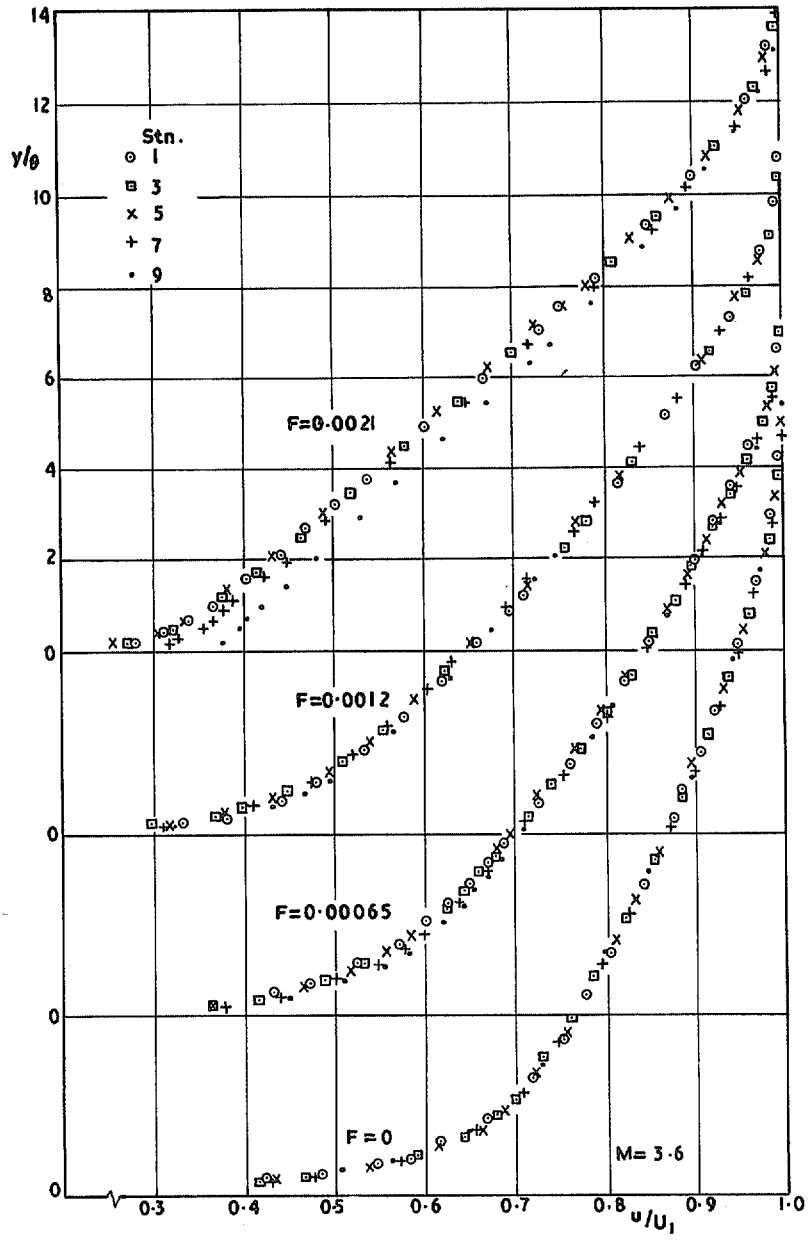

FIG. 12. Velocity profiles at $M = 3{\cdot}6$.

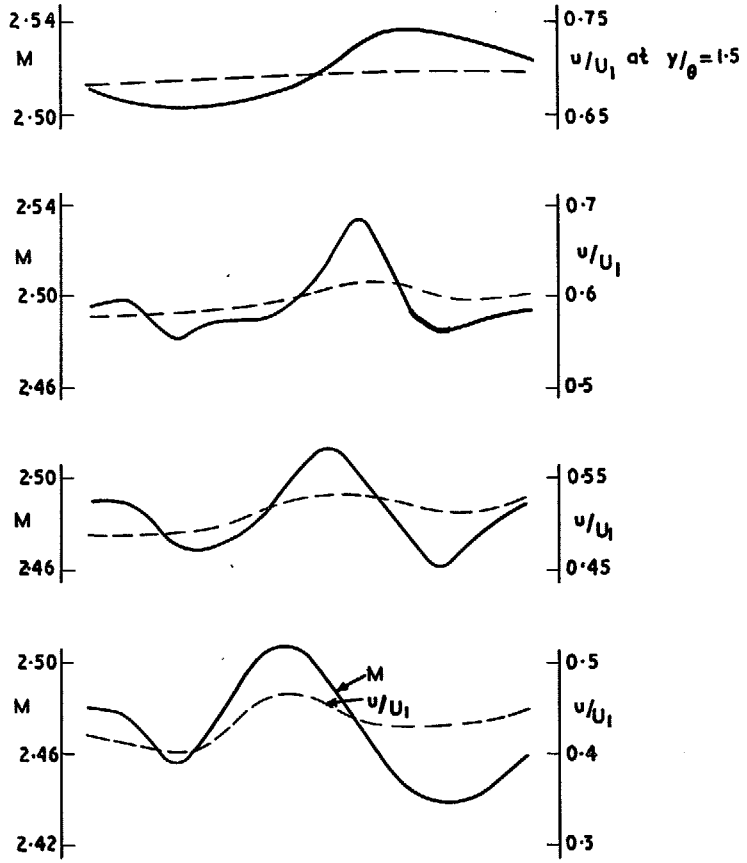

FIG. 13. Correlation of velocity in the boundary layer and in the free stream.

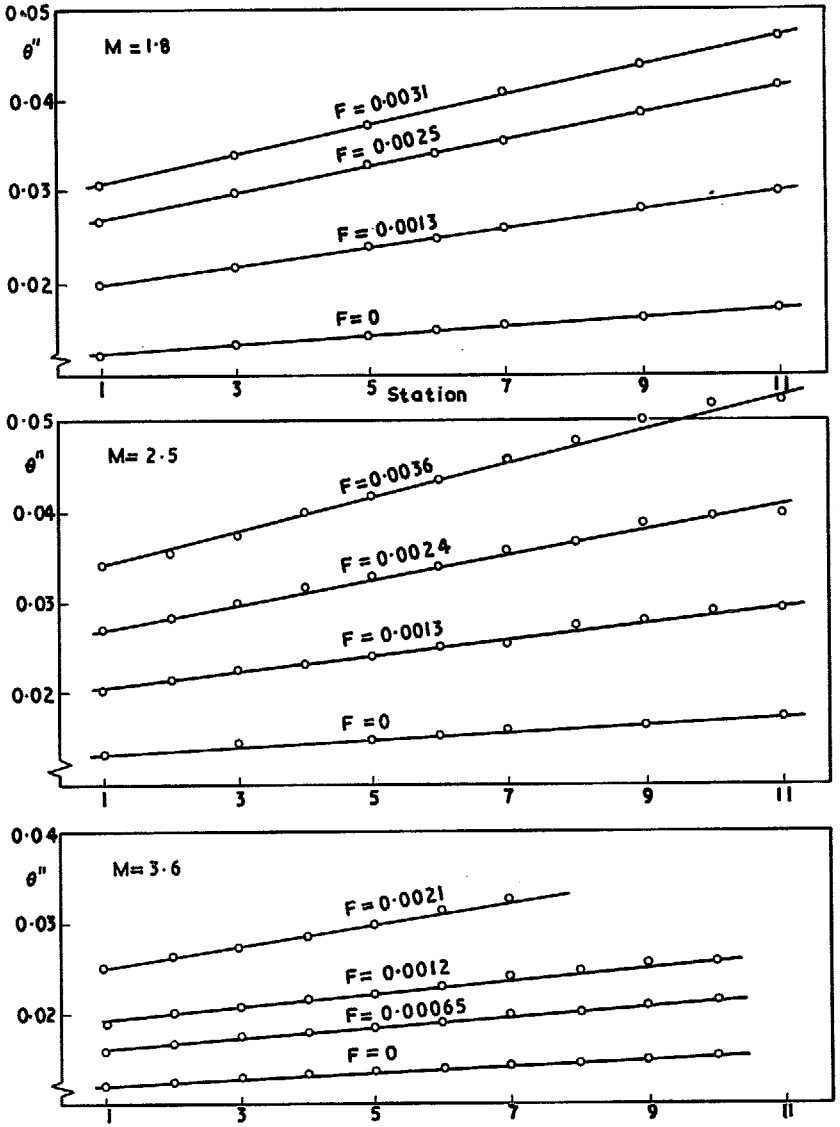

FIG. 14. Momentum growth.

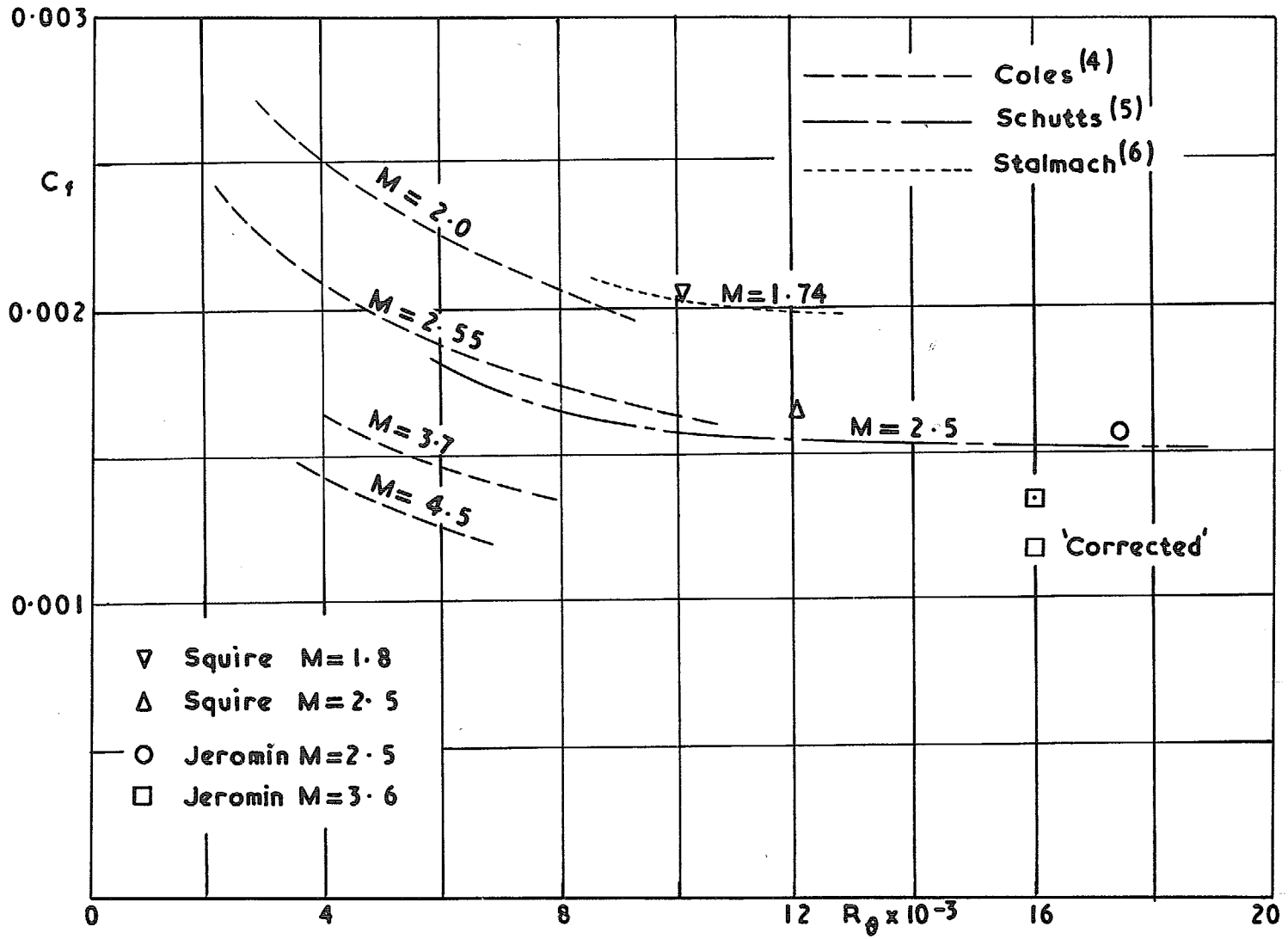

FIG. 15. Skin-friction coefficients with zero blowing.

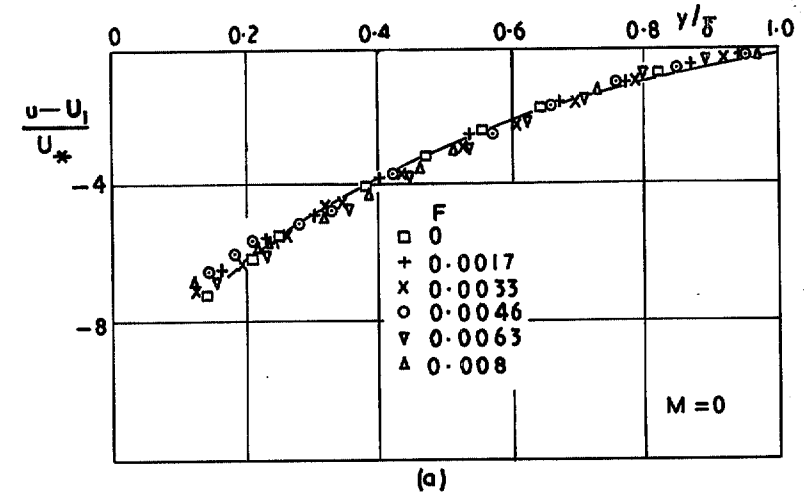

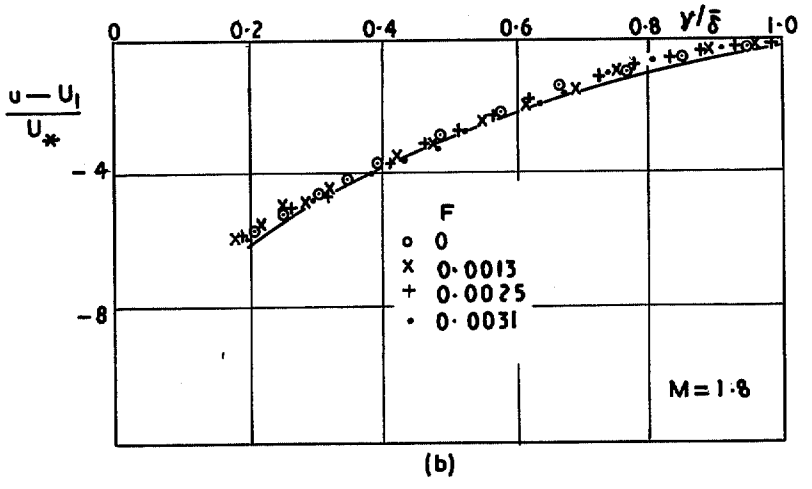

FIG. 16 a & b. Velocity defect law.

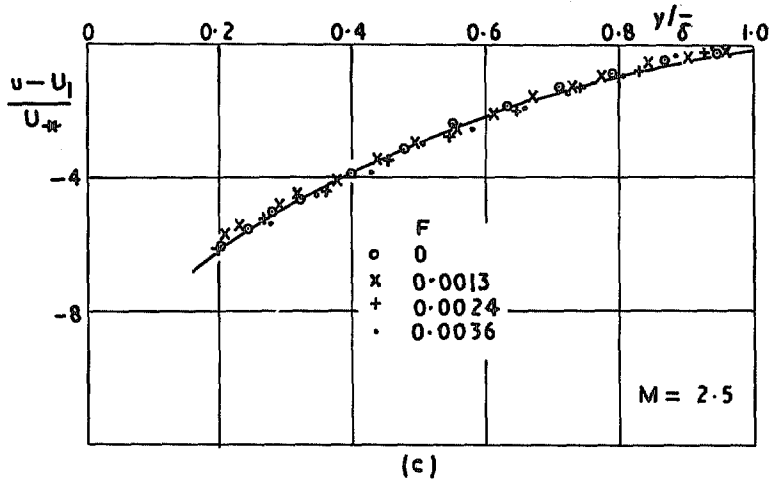

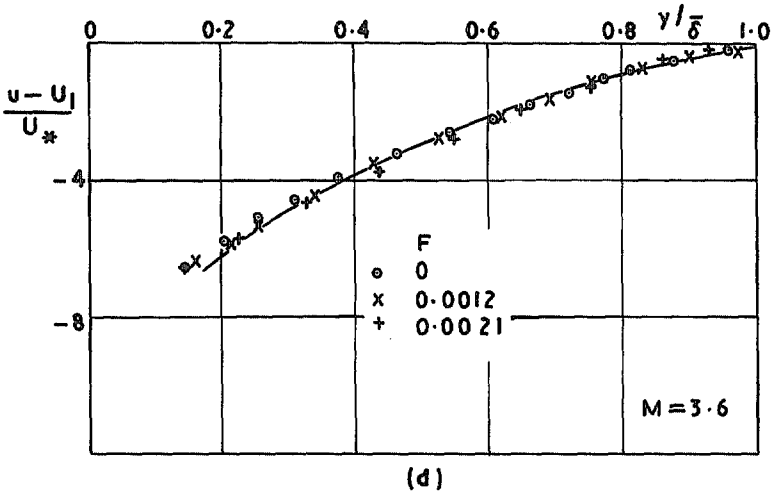

FIG. 16 c & d. Velocity defect law.

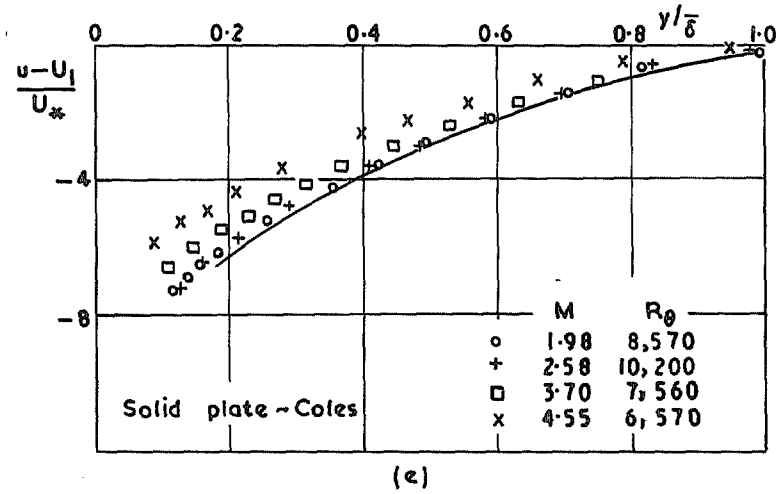

FIG. 16e. Velocity defect law (solid surface).

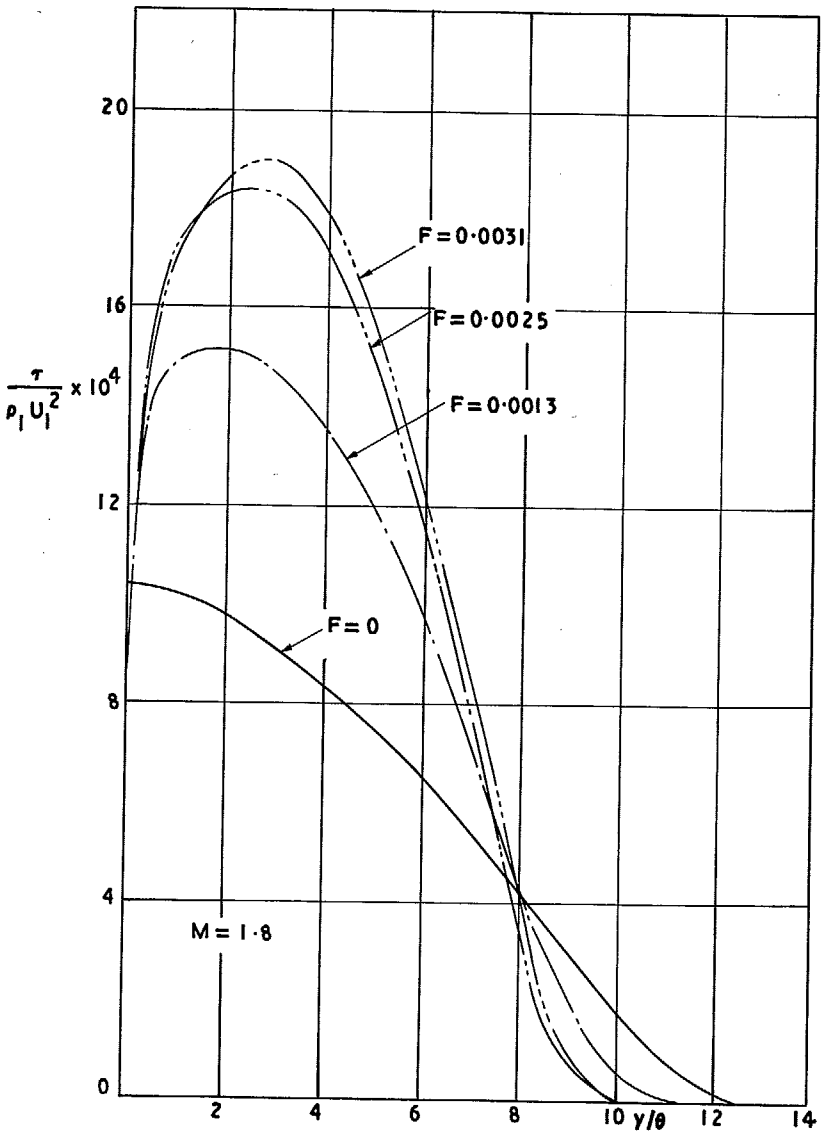

FIG. 17. Shear stress profiles, $M = 1{\cdot}8$.

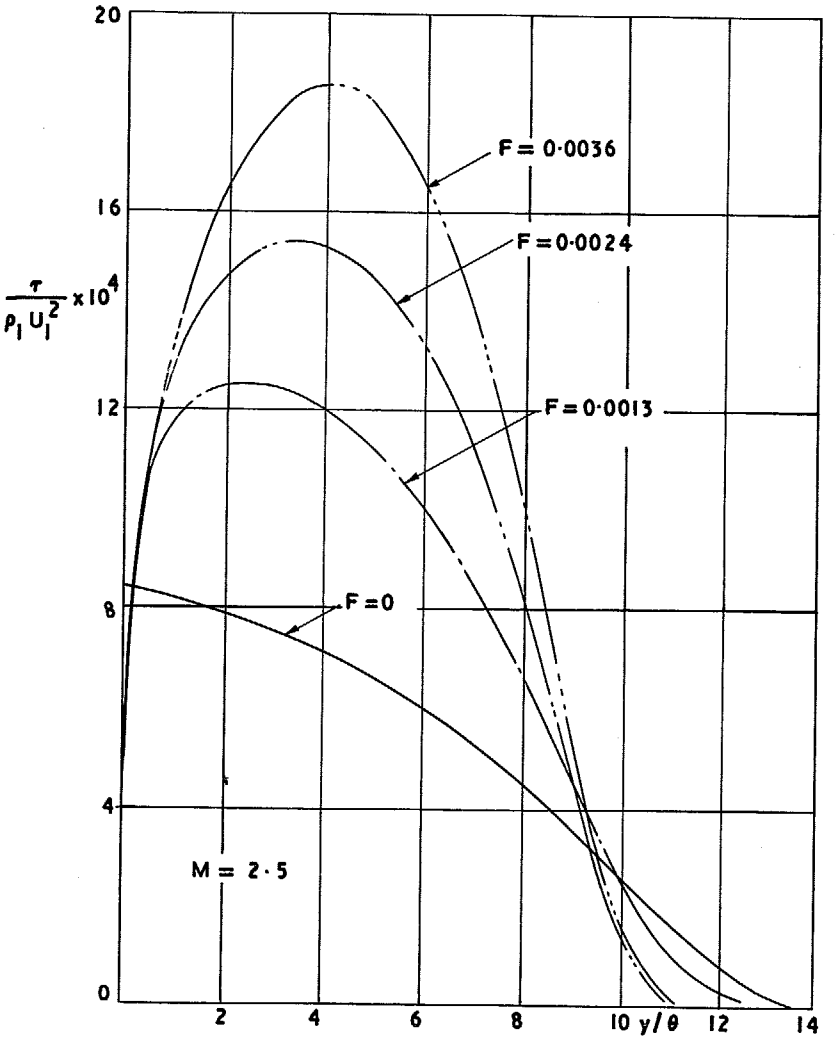

FIG. 18. Shear stress profiles $M = 2{\cdot}5$.

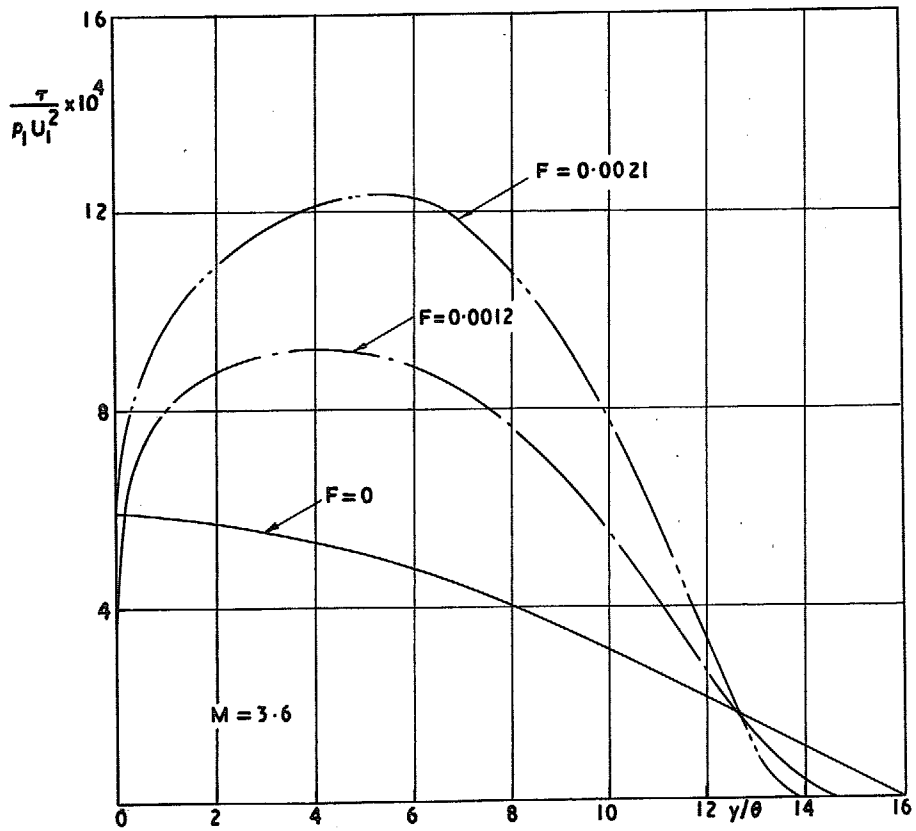

FIG. 19. Shear stress profiles, $M = 3{\cdot}6$.

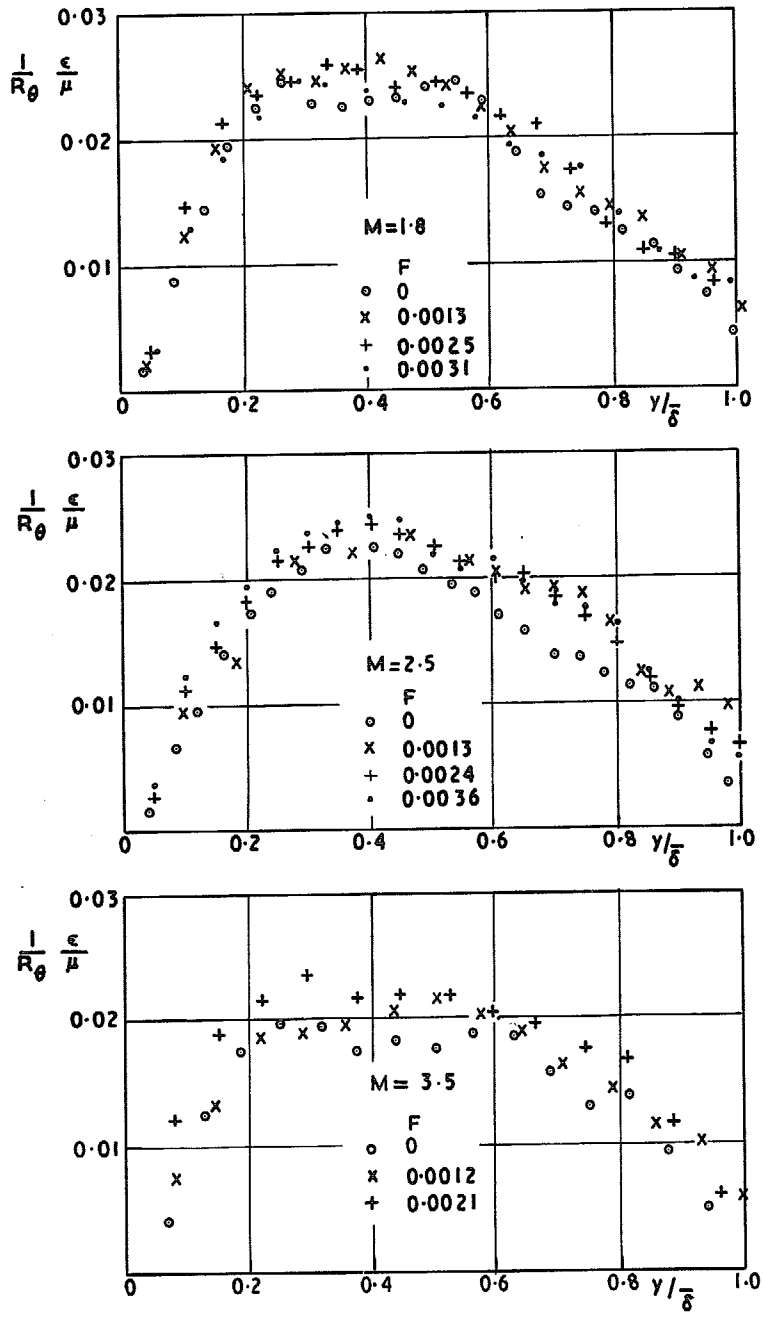

FIG. 20. Eddy-viscosity distributions.

Printed in Wales for Her Majesty's Stationery Office by Allens Printers (Wales) Limited
Dd. 146916 K.5.

Published by
HER MAJESTY'S STATIONERY OFFICE

To be purchased from
49 High Holborn, London WC1
13a Castle Street, Edinburgh EH2 3AR
109 St Mary Street, Cardiff CF1 1JW
Brazennose Street, Manchester M60 8AS
50 Fairfax Street, Bristol BS1 3DE
258 Broad Street, Birmingham 1
7 Linenhall Street, Belfast BT2 8AY
or through any bookseller

R. & M. No. 3627

SBN 11 470327 2